Published in final edited form as:
Prog Neuropsychopharmacol Biol Psychiatry. 2014 April 3; 50: 53–65. doi:10.1016/j.pnpbp.2013.12.003.

Morphine-induced trafficking of a mu-opioid receptor interacting protein in rat locus coeruleus neurons

Kellie M. Jaremko[1,*], **Nicholas L. Thompson Jr.**[1,*], **Beverly A. S. Reyes**[1], **Jay Jin**[2], **Brittany Ebersole**[2], **Christopher B. Jenney**[3], **Patricia S. Grigson**[3], **Robert Levenson**[2], **Wade H. Berrettini**[4], and **Elisabeth J. Van Bockstaele**[1]

[1]Department of Pharmacology and Physiology, Drexel University College of Medicine, Philadelphia, PA 19102

[2]Department of Pharmacology, Penn State College of Medicine, Hershey, PA 17033

[3]Department of Neural and Behavioral Sciences, Penn State College of Medicine, Hershey, PA 17033

[4]Department of Psychiatry, Center for Neurobiology and Behavior, University of Pennsylvania School of Medicine, Philadelphia, PA 19104

Abstract

Opiate addiction is a devastating health problem, with approximately 2 million people currently addicted to heroin or non-medical prescription opiates in the United States alone. In neurons, adaptations in cell signaling cascades develop following opioid actions at the mu opioid receptor (MOR). A novel putative target for intervention involves interacting proteins that may regulate trafficking of MOR. Morphine has been shown to induce a re-distribution of a MOR-interacting protein Wntless (WLS, a transport molecule necessary for secretion of neurotrophic Wnt proteins), from cytoplasmic to membrane compartments in rat striatal neurons. Given its opiate-sensitivity and its well-characterized molecular and cellular adaptations to morphine exposure, we investigated the anatomical distribution of WLS and MOR in the rat locus coeruleus (LC)-norepinephrine (NE) system. Dual immunofluorescence microscopy was used to test the hypothesis that WLS is localized to noradrenergic neurons of the LC and that WLS and MOR co-exist in common LC somatodendritic processes, providing an anatomical substrate for their putative interactions. We also hypothesized that morphine would influence WLS distribution in the LC. Rats received saline, morphine or the opiate agonist [D-Ala2, N-Me-Phe4, Gly-ol5]-enkephalin (DAMGO), and tissue sections through the LC were processed for immunogold-silver detection of WLS and MOR. Statistical analysis showed a significant re-distribution of WLS to the plasma membrane following morphine treatment in addition to an increase in the proximity of gold-silver labels for MOR and WLS. Following DAMGO treatment, MOR and WLS were predominantly localized within the cytoplasmic compartment when compared to morphine and control. In a separate cohort of rats, brains were obtained from saline-treated or heroin self-administering male rats for pulldown co-immunoprecipitation studies. Results showed an increased association of WLS and MOR following heroin exposure. As the LC-NE system is

Corresponding Author: Beverly A. S. Reyes, D.V.M., Ph.D. Department of Pharmacology and Physiology, Drexel University College of Medicine, Philadelphia, PA 19102, Voice: (215) 762-4932, FAX: (215) ask Carmen tomorrow, Beverly.Reyes@drexelmed.edu.
*Kellie M. Jaremko and Nicholas L. Thompson Jr. contributed equally to this work.

important for cognition as well as decisions underlying substance abuse, adaptations in WLS trafficking and expression may play a role in modulating MOR function in the LC and contribute to the negative sequelae of opiate exposure on executive function.

Keywords

Wntless; g-protein receptor; trafficking; norepinephrine; electron microscopy; confocal microscopy

1.1 Introduction

Opioids are a class of drugs that are the most effective analgesics known for many types of pain. However, their clinical utility is limited by tolerance and the propensity for addiction. Opioid addiction afflicts approximately 2 million people in the United States (SAMHSA, 2011). Heroin and non-medical use of prescription opioids rank among the top drugs of dependence that contribute significantly to the 193 billion dollars/year cost of addiction (United States Department of Justice, 2011). Worldwide the estimated annual prevalence of illicit opioid use is a staggering 26–36 million or roughly 0.6–0.8% of the total population (UNODC, 2012). Opioid detoxification, substitution, and maintenance paradigms are the current mainstay of treatment but despite these efforts, opioid abuse and related overdose has continued to escalate in the past decade (CDC, 2012). Novel targets for opioid abuse and elucidating the neuronal pathways that perpetuate substance abuse are needed.

Previous studies have reported conflicting results concerning the effect of chronic morphine on MOR density (Pert et al., 1975; Castelli et., 1997 al., 1997; Petruzzi et al). The magnitude of change and inconsistency between reports has led to the hypothesis that tolerance and dependence are not readily explained by changes in receptor density (Fleming, 1995). Despite a number of putative mechanisms that have been put forth, current studies have failed to identify any single regulatory mechanism underlying tolerance to opioids (Christie, 2008) suggesting that opioid tolerance is a complex, multifaceted process involving the interplay of multiple regulatory mechanisms occurring both at the cellular and circuit level (Williams et al., 2013). Using fluorescence recovery after photobleaching, the movement of MORs on the plasma membrane was found to be agonist-dependent (Saulière-Nzeh et al., 2010). Morphine-bound receptors were more restricted to the membrane, whereas [D-Ala^2, N-MePhe^4,Gly-ol5]enkephalin (DAMGO)-bound receptors either moved freely or were restricted, possibly to clathrin-coated pits. As a partial agonist, morphine does not show significant internalization (Keith et al., 1996, Kovoor et al., 1998, Van Bockstaele and Commons, 2001) compared to etorphine and DAMGO that show robust desensitization and internalization in response to agonist treatment (Bohm et al., 1997, Van Bockstaele and Commons, 2001, Blanchet et al., 2003, Johnson et al., 2006, Virk and Williams, 2008, Wang et al., 2008). The dynamic regulation of MORs at the plasma membrane following acute and chronic administration of opioids may therefore direct downstream signaling (for review see, Williams et al., 2013).

A novel target potentially regulating MOR involves G-protein coupled receptor interacting proteins (GIP) (Bockaert et al., 2004, Milligan, 2005, Ritter and Hall, 2009, Bockaert et al., 2010). Recently, a MOR interacting protein (MORIP) has been identified, the mammalian ortholog of Drosophila Wntless (WLS)/Evi/Sprinter or GPR177 (Jin et al., 2010a, Jin et al., 2010b) WLS may possibly serve as a substrate underlying alterations in neuronal structure, synaptic organization and molecular adaptations characteristic of opioid dependence (Jin et al., 2010a, Jin et al., 2010b, Reyes et al., 2010a, Reyes et al., 2011). WLS contains four (Goodman et al., 2006), seven (Banziger et al., 2006) or eight (Bartscherer et al., 2006)

membrane spanning domains and is essential in mediating the secretion of Wnt signaling proteins (Banziger et al., 2006, Bartscherer et al., 2006). We have previously demonstrated with immunoelectron microscopy that WLS and MOR differentially interact after opioid agonist exposure in rat striatal neurons (Reyes et al., 2011). In those studies, morphine caused a marked shift in WLS from the cytoplasm to the plasma membrane, where it co-localized with MOR.

Morphine-induced cellular and molecular adaptations in noradrenergic neurons of the locus coeruleus (LC) have long been recognized and robustly investigated (Williams et al., 2013). The LC is a compact, homogeneous norepinephrine (NE)-containing nucleus that innervates the entire neuraxis through a divergent efferent system. It is the sole source of NE in many forebrain regions that have been implicated in cognition (e.g., cortex and hippocampus (Foote et al., 1983) and its rate of discharge is positively correlated to behavioral and electroencephalographic indices of arousal (Foote et al., 1980, Aston-Jones and Bloom, 1981b, Aston-Jones and Bloom, 1981a, Page and Valentino, 1994, Berridge and Waterhouse, 2003). Given the opiate-sensitivity of the LC and the well-defined molecular and cellular adaptations of LC noradrenergic neurons following opiate exposure, we sought to investigate the distribution of WLS with respect to MOR in this brain region. In addition, we also examined whether morphine causes a re-distribution of WLS in LC neurons when compared to saline or DAMGO using high resolution immunoelectron microscopic analysis. Finally, we investigated whether heroin exposure caused an increase in MOR/WLS protein interactions using co-immunoprecipitation analysis.

2. Methods

2.1 Subjects

Twelve adult male Sprague-Dawley rats (Harlan Sprague Dawley Inc., Indianapolis, IN, USA; 250–270g) housed two to three to a cage (20°C, 12-h light, 12-h dark cycle lights on 0700) were used in this study. They were allowed ad libitum access to standard chow and water. All procedures were approved by The Institutional Animal Care and Use Committee at Thomas Jefferson University and Penn State College according to the revised *Guide for the Care and Use of Laboratory Animals* (1996), The Health Research Extension Act (1985) and the PHS Policy on Humane Care and Use of Laboratory Animals (1986). All efforts were made to utilize only the minimum number of animals necessary to produce reliable scientific data, and experiments were designed to minimize any animal distress.

2.2 Drug treatment

Adult male rats received intracerebroventricular (i.c.v.) injections of morphine (Sigma-Aldrich Co., St. Louis, MO, USA) dissolved in 0.9% saline to a concentration of 10 mg/ml and administered at 1.0 μg/kg (n =5), 0.9% saline in a volume of 25 μl/kg (n = 5) or DAMGO (Tocris Bioscience, Ellsville, MO, USA) at 5μg/kg body weight (n = 5). Rats were anesthetized with isoflurane (Abbott Laboratories, North Chicago, USA, IL; 0.5–1.0%, in air) via a specialized nose cone affixed to the stereotaxic frame (Stoelting Corp., Wood Dale, IL, USA) and placed in a stereotaxic apparatus for surgery. Micropipettes (Kwik-Fil, 1.2 mm outer diameter; World Precision Instruments, Inc., Sarasota, FL, USA) with tip diameters of 20–25 μm were filled with saline, morphine or DAMGO. The tips of the micropipettes were placed at the following coordinates, 3.5 mm posterior from bregma, 1.4 mm medial/lateral, 3.7 mm ventral from the top of the skull. The stereotaxic coordinates of the injection sites were based on the rat brain atlas of Paxinos and Watson (Paxinos and Watson, 1986). Saline, morphine or DAMGO was injected using a Picospritzer (General Valve Corporation, Fairfield, NJ, USA) at 24–26 psi and over a 10 min period. Pipettes were left at the site of injection for 5 min following drug or vehicle administration.

Thirty minutes following i.c.v. injections of saline, morphine or DAMGO, rats were euthanized. The time of euthanasia post-treatment was selected based on previous studies from our group (Van Bockstaele and Commons, 2001, Jin et al., 2010a, Reyes et al., 2011). Using an *in vitro* technique in MOR expressing human embryonic kidney 293 cells a MOR/WLS complex was detected 1 hour following DAMGO treatment (Jin et al., 2010a). Moreover, another *in vivo* study using high resolution electron microscopy in rat brain showed significant MOR internalization 30 min following treatment with the opiate agonist, etorphine (Van Bockstaele and Commons, 2001), as well as with changes in MOR and WLS localization in rat striatal neurons (Reyes et al., 2011). Finally, it is well known that agonist-induced trafficking and up-regulation may occur rapidly from seconds to minutes (Zigmond et al., 1982, Norgauer et al., 1991) and the time point of 30 minutes was considered to be optimal for detecting changes in trafficking patterns.

2.3 Immunoblotting

Tissues were harvested from adult Sprague-Dawley rats, frozen on dry ice, and thawed prior to homogenization in lysis buffer (Hannan et al., 2008). Brain regions were dissected and lysates prepared immediately after animals were sacrificed. Crude membrane fractions from rat brain lysates were prepared as previously described (Karpa et al., 1999). Membrane fractions were separated on SDS-containing10% polyacrylamide gels, then transferred to polyvinylidine difluoride (PVDF) membranes. Filters were blocked for 2 hour in Tris-buffered saline with Tween-20 (TBS-T; 20 mM Tris,pH 7.4;, 275 mM NaCl, 3 mM KCl, 1% Tween-20) containing 10% dry milk. Blots were incubated with chicken anti-WLS antibodies (Gene-Tel Laboratories, Madison, WI, USA; 1:5,000–1:2,500 dilution) for 1 hour, then horseradish-peroxidase (HRP)-conjugated donkey anti-chicken secondary antibodies (1:15,000) for 1 hour. Immunoreactivity was detected using an Enhanced Chemiluminescence (ECL) Plus kit (GE Healthcare, Piscataway, NJ).

2.4 Immunohistochemistry

For all experiments the primary antibodies were as follows: chicken anti-WLS antiserum (Gene-Tel Laboratories, Madison, WI, USA; 1:1000), mouse anti-tyrosine hydroxylase (TH; Immunostar Inc., Hudson, WI, USA; 1:1,000), and either rabbit or guinea pig anti-MOR (Chemicon/Millipore, Billerica, MA, USA; 1:1000). Thirty minutes following injection, rats were deeply anesthetized with sodium pentobarbital (80 mg/kg; Ovation Pharmaceuticals, Inc., Deerfield, IL, USA) and transcardially perfused through the ascending aorta with 10 ml heparinized saline followed by 25 ml of 3.75% acrolein (Electron Microscopy Sciences, Fort Washington, PA, USA), and 50 ml of 2% formaldehyde in 0.1 M phosphate buffer (PB; pH 7.4). The brains were removed immediately after perfusion fixation, sectioned into 1–3 mm coronal slices and post-fixed in the same fixative overnight at 4°C.

Forty micron-thick coronal sections through the rostrocaudal extent of LC (Paxinos and Watson, 1986) were cut using a Vibratome (Technical Product International, St Louis, MO, USA) and rinsed extensively in 0.1 M PB and 0.1 M TBS (pH 7.6). Sections were placed for 30 min in 1% sodium borohydride in 0.1 M PB to reduce amine-aldehyde compounds. The tissue sections were then incubated in 0.5% bovine serum albumin (BSA) in 0.1 M TBS for 30 min. Subsequently, sections were incubated in primary antibody solution, as specified below for each experiment. Incubation time was 15–18 hours in a rotary shaker at room temperature. Thorough rinses in 0.1 M TBS were conducted following each incubation procedure.

Primary antibody incubation of WLS, TH and MOR (guinea pig) was done in a 0.1% BSA, 0.5% triton, and 0.1M TBS overnight. Detection of WLS by immunoperoxidase was conferred with a donkey anti-chicken IgY biotin conjugated secondary antibody (Jackson

Immunoresearch Laboratories Inc., West Grove, PA, USA; 1:400) in 0.1% BSA, 0.5% triton, and 0.1M TBS solution for 30 minutes at room temperature. Then an avidin-biotin complex solution (Vector Laboratories, Burlingame, CA, USA) was used for another 30 minutes. The peroxidase reaction product was then visualized using 0.02% 3-3' diaminobenzidine (DAB; Aldrich, Milwaukee, WI, USA) plus 10 mL of 30% hydrogen peroxide in 0.1 M TBS for 7 minutes. Tissue sections underwent serial dehydration, were mounted on slides, and cover slipped using Permount or DPX (Sigma Aldrich, St. Louis, MO, USA). Visualization and image capture was done with Olympus BX51 microscope in combination with Advanced Spot software and camera (v4.1, model # 2.2.1, 2004, Diagnostic Instruments Inc., Sterling Heights, MI, USA). Fluorescent detection of WLS, MOR, and TH was accomplished by secondary antibody incubation for 2–3 hours, covered from light, at room temperature, with FITC conjugated donkey-anti guinea pig IgG for MOR detection, TRITC conjugated donkey-anti chicken IgY for WLS, Cy5 donkey-anti mouse for TH detection conjugated detection (Jackson Immunoresearch, West Grove, PA, USA; 1:200). Tissue sections were mounted on slides, and cover slipped using fluoromount, or DAPI mounting medium (Sigma Aldrich). Slides were then viewed using a fluorescent confocal microscope, and images were prepared using the Zeiss LSM Image Browser and Adobe Photoshop. Analysis of the number of cells (mean ± SEM) labeled with MOR, WLS, TH, and colocalization was done for 4 non-consecutive LC slices from naïve male rats.

2.5 Immuno-electron microscopy

For high-resolution immune-EM, WLS was visualized using the immunogold-silver enhancement technique, with or without TH labeled with peroxidase, in parallel for control and experimental animals, using the same reagents.

Gold and peroxidase labeling has been done by our group as described previously (Reyes et al., 2007, Scavone and Van Bockstaele, 2009). Primary antibody incubation with WLS at 1:1000 in 0.1% BSA and 0.1M TBS, and in some sections with TH (1:1000) was done overnight. Then tissue sections were rinsed three times with 0.1 M TBS, followed by biotinylated anti-mouse for TH peroxidase labeling at 1:400 (Vector Laboratories, Burlingame, CA, USA) following the same protocol detailed above for light microscopy with ultimate DAB exposure for 1–2minutes. Immune-gold visualization was processed with a 10-minute incubation in a 0.2% gelatin-PBS and 0.8% BSA buffer followed by a two-hour incubation in goat anti-chicken IgY conjugate in 1 nm gold particles (1:50) (Amersham Bioscience Corp., Piscataway, NJ, USA) at room temperature. Biotinylated anti-mouse for TH labeling at 1:400 (Vector Laboratories, Burlingame, CA, USA), and an avidin-biotin complex solution (Vector Laboratories) was used. The peroxidase reaction product was then visualized using 0.02% DAB plus 10 mL of 30% H2O2 in 0.1 M TBS for 1–2minutes. Sections were then rinsed in buffer containing the same concentration of gelatin and BSA as above. Following rinses with 0.01 M PBS, sections were then incubated in 2% glutaraldehyde (Electron Microscopy Sciences) in 0.01 M PBS for 10 min. The conjugated gold particles were intensified by incubation in a silver enhancement solution (Amersham Bioscience Corp.). The optimal times for silver enhancement were determined by empirical observation for each experiment and ranged between 8 and 10 min. Following intensification, tissue sections were rinsed in 0.2 M citrate buffer and 0.1 M PB, and fixed in 2% osmium tetroxide (Electron Microscopy Sciences) in 0.1 M PB for 1 h, washed in 0.1 M PB, dehydrated in an ascending series of ethanol followed by propylene oxide and flat embedded in Epon 812 (Electron Microscopy Sciences; (Leranth and Pickel, 1989b) between two sheets of Aclar plastic (Honeywell, Pottsville, PA, USA).

Thin sections of approximately 50–100 nm in thickness were cut with a diamond knife (Diatome-US, Fort Washington, PA, USA) using a Leica Ultracut (Leica Microsystems, Wetzlar, Germany). Captured images of selected sections were compared with captured light

microscopic images of the block face before sectioning. Sections were collected on copper mesh grids, examined with an electron microscope (Morgagni, Fei Company, Hillsboro, OR, USA) and digital images were captured using the AMT advantage HR/HR-B CCD camera system (Advance Microscopy Techniques Corp., Danvers, MA, USA). Figures were assembled and adjusted for brightness and contrast in Adobe Photoshop CS6 software (Adobe Systems, Inc., San Jose, CA, USA).

Immunogold-silver labeling for WLS appeared as intense black electron-dense particles and was identified in somata and dendritic processes as we have recently demonstrated(Jin et al., 2010a, Reyes et al., 2010a, Reyes et al., 2011). Selective immunogold-silver labeled profiles were identified by the presence, in single thin sections, of at least two immunogold-silver particles within a cellular compartment (Jin et al., 2010b, Reyes et al., 2010a, Reyes et al., 2011). The criterion of two gold particles as indicative of WLS labeling is conservative and may have led to an underestimation of the number of WLS-labeled profiles. Another factor that may have led to the underestimation of labeled profiles is the limitation of immunocytochemical methods to detect trace amounts of WLS. To circumvent the caveat of incomplete antibody penetration which is inherent to pre-embedding technique, tissue sections were collected close to the plastic-tissue interface and to ensure that the immunogold labeling was detectable in all sections analyzed. Additionally, unbiased stereological methods were not used for counting labeled profiles, and the results of the numerical analysis can only be considered to be an estimate of the numbers of synapses and labeled profiles.

2.5.1 Sequential immunogold-silver labeling—Following the procedure for dual immunogold-silver labeling that we recently described (Jin et al., 2010b, Reyes et al., 2010a, Reyes et al., 2011), WLS and MOR were identified using sequential immunogold-silver labeling. Tissue sections were incubated for 15–18 hours in a cocktail containing chicken anti-WLS antiserum (Gene-Tel Laboratories) at 1:1000 and rabbit anti-MOR (Immunostar) at 1:2000 in 0.1%BSA and 0.1M TBS. Thereafter, sections were rinsed extensively in 0.1 M TBS and 0.2% BSA in 0.01 M PBS followed by incubation in goat anti-rabbit IgG ultra-small conjugate (1:100; Amersham Bioscience Corp.) at room temperature for 8 hours. Tissue sections were rinsed six times in 0.2% BSA-0.01 M PBS and twice in 0.1 M PB. Pre-enhancement washings were done with Enhancement Conditioning Solution (ECS; Amersham Bioscience Corp.) followed with the first silver enhancement (300 μl R-Gent SE-EM enhancement mixture; Amersham Bioscience Corp.) for 90 min. Subsequently, tissue sections were rinsed in 0.2 M citrate buffer, four times in ECS and two times in 0.1 M PB and were incubated in goat anti-chicken IgG ultra-small conjugate (1:100; Amersham Bioscience Corp.) at room temperature for 8 hours followed by rinses with 0.2% BSA-0.01 M PBS and 0.1 M PB. Then, sections were incubated in 2.5% glutaraldehyde (Electron Microscopy Sciences) in 0.01 M PBS for 2 hours followed by extensive rinses with 0.1 M PB and distilled water. The second silver enhancement (300 μl R-Gent SE-EM enhancement mixture; Amersham Bioscience Corp.) was performed for 60 min. Tissues sections were washed extensively with distilled water and 0.1 M PB. All washes were done at 10 min-intervals. Following washes, tissue sections were incubated in 2% osmium tetroxide (Electron Microscopy Sciences) in 0.1 M PB for 1 h, washed in 0.1 M PB, dehydrated in an ascending series of ethanol followed by propylene oxide and flat embedded in Epon 812. Sectioning with a diamond knife, examining with an electron microscope and obtaining digital images followed standard protocols described earlier.

2.6 Controls and data analysis

Every fourth adjacent section through the LC was included in immunohistochemical staining for WLS with MOR or TH. Some sections were processed in parallel with the rest of the

procedures identical but the primary antiserum was omitted. Sections processed in the absence of primary antibody did not exhibit immunoreactivity (Jin et al., 2010b, Reyes et al., 2010a, Reyes et al., 2011). For quantitative single and dual immunogold quantification tissue sections were taken from three rats per group with the good preservation of ultrastructural morphology and with clearly apparent immunocytochemical labeling. At least 9 grids containing 5 to 8 thin sections each were collected from at least two plastic-embedded sections of the LC from each animal. The quantification of MOR, TH and WLS-immunolabeled profiles were carried out at the plastic-tissue interface to ensure that immunolabeling was detectable in all sections used for analysis (Chan et al., 1990). To determine whether levels of spurious silver grains could contribute to false positives, blood vessels and myelinated axons (structures that should not contain WLS immunolabeling) were counted in random ultrathin sections. Minimal spurious labeling was identified. Therefore, the criteria for considering a process as immunolabeled was defined by the presence of at least 2–3 silver grains in a cellular profile. The identification of cellular elements was based on the standard morphological criteria (Peters et al., 1991, Peters and Palay, 1996). WLS and MOR immunolabeling was identified as either cytoplasmic or plasmalemmal. If the immunogold-silver grains were associated with the plasma membrane they were classified as plasmalemmal and if the immunogold-silver grains were not in contact with the plasma membrane they were classified as cytoplasmic. A total of 2735 dendritic profiles exhibiting WLS immunoreactivity from all groups were used in the analysis. Specifically, the dendritic profiles were randomly obtained from each rat and ranged in number from 119–211 dendritic profiles per animal. Statistical analysis of the number of profiles obtained showed no significant difference in the number of dendritic profiles sampled per group (saline = 147.67 ±26.15; morphine 157.67 ±39.10; DAMGO = 150.5 ±33.41) and examined between groups. The analysis of WLS internalization in various groups studied was quantified by calculating the ratio of cytoplasmic to total immunogold-silver particles for each singly immunolabeled dendritic profile in individual rats. All the data gathered and analyzed were obtained per animal and the average of three animals was calculated. The cross sectional size of each dendritic profile was obtained using Image J software (NIH). In addition, as with previous studies from our group (Reyes et al., 2006, Reyes et al., 2008, Wang et al., 2009), care was taken to ensure that control and experimental groups contained similarly sized profiles. We did not observe any statistical difference in the size of profiles analyzed in any group examined as we have recently reported (Scavone and Van Bockstaele, 2009, Reyes et al., 2011). For the sequential immunogold-silver labeling, semi-quantitative analysis was carried out by randomly obtaining the ratio of cytoplasmic to total immunogold-silver particles for WLS and MOR in a dendritic profile exhibiting both WLS and MOR immunoreactivities. Labeling for each protein of interest was differentiated by electron dense particle size and this resulted in two groups of silver-enhanced particles: smaller particles that were enhanced once and larger particles that were enhanced twice (Yi et al., 2001, Jin et al., 2010a, Reyes et al., 2010a, Reyes et al., 2011). Dual immunogold–silver particles were readily discernible from one another with MOR as large (cross sectional diameter >0.05 microns) and WLS as small (cross sectional diameter <0.05 microns) gold–silver particles, as established in prior studies by our group (Jin et al., 2010a). Image J was used to measure distances between MOR and WLS immunogold silver particles. All numerical data is represented as mean ± SEM, unless otherwise specified. Statistical analysis was done with GraphPad Prism 5 statistical software (GraphPad Software, Inc. 2012; La Jolla, CA, USA) to calculate one-way ANOVA with post-hoc Tukey tests or independent *t*-test, as necessary. Two tailed tests were used and significance set as $p < 0.05$.

2.7 Saline and heroin self-administration studies

In another in vivo experiment, adult male rats self-administered either saline or heroin. The subjects were 24 naïve, male, Sprague Dawley rats. Rats were housed individually in wire bottom cages, in a humidity and temperature-controlled (21°C) animal care facility with a standard 12/12 h light/dark cycle (lights on at 0700h). All rats were given *ad lib* access to Purina Rodent Diet 5001 and to water except where noted. All experimental protocols complied with National Institutes of Health Animal Care Guidelines and were approved by the Pennsylvania State University Institutional Animal Care and Use Committee.

2.7.1 Surgery—Rats were anesthetized with a Ketamine and Xylazine mixture and a jugular catheter implanted as described (Grigson and Twining 2002; Jones et al., 2002; Twining et al., 2009). Briefly, catheters were implanted into the right external jugular vein with tubing extending subcutaneously past the neck to a capped cannula exiting dorsal to the shoulder blades. Patency of catheters was maintained by daily flushing with heparinized saline (0.2 ml of 30 IU/ml heparin) and periodically verified by intravenous administration of 0.2 ml of the short-acting anesthetic, 1% Diprivan (Propofol, Fresenius Kabi, Lake Zurich, IL).

2.7.2 Apparatus—Each rat was trained in one of 12 identical operant chambers (Med Associates, St. Albans, VT) measuring 30.5×24.0×29.0 cm and housed in light and sound attenuating cubicles. All chambers have clear Plexiglas tops, fronts, and backs. Sidewalls are aluminum. The floors consist of 19 stainless steel rods (4.8 mm) spaced 1.6 cm apart center to center. Each chamber is equipped with three retractable operant sipper tubes (spouts) that enter the left side of the chamber through 1.3 cm diameter holes spaced 8.0 cm center to center. A stimulus light is located 6 cm above each spout. A lickometer circuit is used to record spout licks. Each chamber is equipped with a house light (25 W), a tone generator (Sonalert Time Generator, 2900 Hz; Allied Electronics, Fort Worth, Texas), and a white noise speaker (75 dB). Self-administration reinforcement is controlled by an electronic circuit operating a syringe pump (Med Associates). Collection of the data and control of chamber events are performed on-line using a Pentium-based computer. Programs were written in Medstate notation language (Med Associates).

2.7.3 Coupling assembly—Prior to each self-administration session, a coupling assembly was attached to the catheter assembly on the back of each rat. The coupling assembly consisted of a metal spring attached to a threaded metal spacer to provide protected passage of the catheter tubing (Tygon, US Plastic Corp., Lima, Ohio) down the center of the apparatus to the animal. The assembly was attached to a counterbalanced swivel (Instech, Plymouth Meeting, PA) connected to a syringe pump outside of the cubicle.

2.7.4 Testing—Phase I. Taste-drug parings. After habituation to the self-administration chambers, all rats were tested on a tastant/drug pairing schedule as described (Grigson and Twining 2002). Basically, rats were trained for one trial per day for three consecutive days. Each trial allowed for the opportunity to lick 0.15% saccharin from the left empty spout of the self-administration chamber for 5 min with the houselight and white noise on. The left empty spout then retracted and the center and right empty spouts advanced. This was followed by 6 h access to heroin (n=16) or saline (n=8) on a FR10 schedule of reinforcement where 10 licks on the right, empty spout (the “active” spout) led to an iv infusion of heroin (0.06 mg in 0.2 ml saline) or saline only over 6 s. Heroin or saline infusion is signaled by retraction of the spout, extinguishing the stimulus light and onset of the houselight and a tone for 20 s. The middle empty spout operant is referred to as the “inactive” spout and responses on this operant are without consequence. The continuation of the trial is signaled

by extinction of the houselight, and illumination of a stimulus light located above the right active empty spout operant.

Phase II. Assessment of 'addiction-like' behavior. Immediately following Phase I testing, the gustatory cue was no longer provided and all rats were given the opportunity to self-administer heroin or saline, as per their previous group assignment, on a FR10 schedule, but using a slightly different procedure (Puhl et al., 2011). Basically, during each trial, rats were allowed to self-administer heroin for three 40 minute drug periods, interspersed with two 15 minute signaled drug non-availability (SNA) periods. All rats were tested once per day, Monday through Friday, with weekends off to avoid overdose. After 24 trials, rats were tested for their motivation to take drug using a modified version of the PR schedule used by Piazza (Deroche-Gamonet et al., 2004) and described previously by our lab (Puhl et al., 2011). This was followed by an extinction and reinstatement trial wherein rats were placed in the chambers for 7 h. For the first 6 h, spout responses were not reinforced in order to extinguish drug seeking behavior. At the beginning of the 7^{th} h, each rat received a single computer controlled, non-contingent priming injection of 0.06 mg heroin or saline followed by one h of reinstatement testing on the standard FR10 schedule. This was followed by five days of FR10 self-administration using this variation of the Piazza model.

2.7.5 Heroin addiction-like behaviors—One heroin rat developed an infection during testing and was euthanized. Following the taste-drug pairings, the heroin-treated rats were broken into two groups separated by median number of licks of saccharin. Those falling above median were termed small suppressors (n=7); those falling below were termed large suppressors (n=8). Large suppressors in the saccharin-heroin condition made significantly fewer licks on the saccharin cue than did small suppressors in the saccharin-heroin condition ($P < 0.01$).

During the last fifteen FR trials heroin intake stabilized to an average of 7 infusions per trial with no difference between large and small suppressors. For the PR test, there was no significant difference in break point between heroin groups. During the reinstatement phase of the extinction/reinstatement test, large suppressors relapsed to drug, taking a significantly greater number of infusions than control ($P < 0.05$), but small suppressors did not.

2.7.6 Euthanasia and tissue dissection—Twenty-four h later, the rats were sacrificed by rapid decapitation, brains were removed manually, bisected longitudinally, and the left hemisphere was placed into a solution of 4% formalin for 24 hours. The samples were then transferred to phosphate-buffered saline and maintained at 2–4°C until they were processed at Penn. Tissue from the right hemisphere was dissected into regions of interest including the locus coereleus, nucleus accumbens, ventral tegmental area (VTA), hippocampus, and the prefrontal cortex. These samples were stored in liquid nitrogen and then transferred to a −80°C freezer.

2.7.7 Co-immunoprecipitation—All tissue was suspended in lysis buffer (50 mM Tris-HCl, pH 7.4, 1 mM EDTA, 150 mM NaCl, 1% NP40, 0.25% deoxycholate, 5 mM NaF, 2 mM Na_3VO_4) containing protease inhibitors (complete MINI EDTA free, Roche, Indianapolis, IN), homogenized using a microcentrifuge pestle for 2 minutes and sonicated using a probe sonicator, then centrifuged at 4°C, 13,000 RPM for 20 minutes to remove cellular debris (Petko et al., 2013). LC tissue from three saline and three heroin self-administering rats were separately pooled prior to performing co-immunoprecipitation. Protein concentrations in LC tissue samples were determined as previously described (Jin et al., 2010a,b), and equal amounts of protein were added to each immunoprecipitation reaction. GammaBind G Sepharose beads (GE Healthcare, Uppsala, Sweden) were used to preclear immunocomplexes from LC tissue. Protein-G MAG sepharose beads (GE

Healthcare) were coated with rabbit anti-MOR antibody (AB1580, Millipore, Billerica, MA) according to manufacturer's instructions, then incubated with 1 mg of precleared LC lysate. Proteins were eluted using 1X loading dye (62.5 mm Tris-HCl pH 6.8, 10% glycerol, 2% SDS, 0.025% bromophenol blue, 5% β-mercaptoethanol), and analyzed via SDS-PAGE/ Western blotting using chicken anti-WLS (1:2000; Jin, et. al., 2010a) antibody.

3. Results

3.1 WLS is enriched in locus coeruleus noradrenergic neurons that also express MOR

Consistent with previous studies (Jin et al., 2010b), Western blot analysis of rat brain lysates from cortex, striatum, and brainstem nuclei including the LC, demonstrated robust expression of WLS (Fig. 1 B). Immunoblot blot analysis revealed a diffuse, band migrating between 37 to 50kD consistent with previous reports (Jin et al., 2010b).

Using immunoperoxidase labeling combined with light microscopic analysis in coronal brain sections of naïve male rats, WLS expression was identified specifically in the LC region (Fig. 1 D–E). Immunoreactivity for WLS in the LC was considerably more robust than in neighboring regions of the dorsal pons, such as the superior cerebellar peduncle, that did not exhibit strong WLS immunoreactivity. Tissue sections processed for light microscopic detection (Fig. 1 C) in the absence of the primary antibody directed against WLS revealed a lack of immunocytochemical labeling. These data supported our hypothesis that WLS is highly expressed in the LC region and prompted a more in depth investigation of WLS association with noradrenergic neurons.

Triple labeling immunofluorescence studies were used to examine potential co-localization of WLS with the noradrenergic marker, TH, and MOR in the LC. Tissue sections processed in the absence of each of the primary antibodies for fluorescent microscopy revealed a lack of immunocytochemical labeling and a lack of cross-reactivity between secondary antibodies. We confirmed previous studies showing that MOR is abundant within noradrenergic neurons of the LC (Van Bockstaele et al., 1996, Moyse et al., 1997, Scavone and Van Bockstaele, 2009). Figure 2 presents that TH, WLS and MOR were prominently distributed within the LC (Fig. 2). WLS frequently co-localized with MOR in TH-containing neurons. Overall, approximately half of all LC neurons identified were triple labeled for WLS, MOR, and TH (Fig. 2). Similarly, almost ¾ of all MOR-containing neurons also exhibited immunoreactivity for WLS. However, although MOR and WLS are frequently co-localized to the same neurons, there were some clear examples where individual cells expressed one or the other in noradrenergic cells.

To further define the subcellular distribution of WLS in noradrenergic LC neurons, immunogold-silver detection of WLS was combined with immunoperoxidase labeling of TH. Immunogold–silver labeling of WLS appeared as irregularly shaped black deposits that were localized to dendritic and somatic processes within the LC (Fig. 3). Similar to our previous studies on the localization of WLS in the striatum of rats and mice (Reyes et al., 2010a, Reyes et al., 2011), gold-silver labeling indicative of WLS was observed within the cytoplasm of somatodendritic processes as well as associated with the plasma membrane. Although dual immunoelectron analysis with immunogold labeling for WLS and immunoperoxidase labeling for TH revealed that WLS was frequently localized within noradrenergic dendritic processes, dendritic profiles lacking TH that exhibited WLS immunoreactivity could be seen in portions of the neuropil adjacent to TH/WLS dually labeled neurons in the LC (Fig. 3A). Dendrites solely labeled for WLS were often found to have symmetric synapses indicative of inhibitory contacts (Fig. 3A). The majority of dendritic profiles, however, were dual labeled with approximately 70% of all TH dendrites containing WLS immunoreactivity (Fig. 3B).

3.2 WLS shifts to the plasma membrane following acute morphine treatment

To determine whether opiate agonists influence the cellular distribution of WLS in LC neurons, rats received an acute i.c.v. injection of saline, morphine or DAMGO and the subcellular distribution of WLS was measured by calculating the ratio of the cytoplasmic to total (cytoplasmic and plasmalemmal) labeling. To ensure that results were not biased by differences in gold-silver labeling in different sized dendrites, we quantified the ratio of WLS in cytoplasmic vs. total immunogold–silver particles in large-(>5 μm in perimeter) and small-(<5 μm in perimeter) dendrites. Statistical analysis showed similar ratios across the two populations of differentially sized dendrites and, therefore, all dendrites were pooled for the final analysis.

Immunogold-silver particles indicative of WLS were primarily associated with the cytoplasm of LC dendrites and occasionally on the plasma membrane of control rats that received an i.c.v. injection of saline (Fig. 4A–B). Following DAMGO administration, a MOR agonist known to induce significant MOR internalization (Whistler and von Zastrow, 1999, Bailey et al., 2003), Figure 4E–F show a greater prevalence in the cytoplasmic distribution of WLS. Conversely, morphine treatment induced a shift of WLS to the plasma membrane (Fig. 4C–D).

3.3 WLS and MOR are in close proximity on the plasma membrane of morphine treated rats

Analysis of WLS immunoreactivity using single labeling was important in unequivocally establishing differences in opiate agonist-induced re-distribution of WLS. However, we next sought to define whether WLS re-distribution occurred in dendrites that co-express MOR. To this end, tissue sections were sequentially labeled using a dual immunogold-silver processing approach for MOR and WLS, as previously described (Jin et al., 2010a, Reyes et al., 2011). Obtaining different sized immunogold–silver particles was achieved by incubating with one ultra-small gold conjugate antibody directed against the first antibody, followed by silver enhancement, and then incubating with the second ultra-small gold conjugate directed against the second antibody, followed by additional silver enhancement (Yi et al., 2001). This resulted in two groups of silver-enhanced particles: smaller particles that were enhanced once and larger particles that were enhanced twice (Yi et al., 2001, Jin et al., 2010a, Reyes et al., 2011).

Dual immunogold–silver labeling (large and small gold–silver particles, for MOR and WLS, respectively) that were localized in the same tissue section were readily distinguishable from each other (Fig. 5A–B) Following morphine, large black punctate silver enhanced gold particles, indicative of MOR, appeared on the plasma membrane (Fig. 5C–D) (0.411 ± 0.050) similar to the MOR distribution in saline treated rats (0.441 ± 0.020). As described above, morphine induced a shift in the distribution of WLS from the cytoplasm to the plasma membrane (0.423 ± 0.050). In contrast, DAMGO caused a shift of MOR from the plasma membrane to the cytoplasm (0.687 ± 0.0157). WLS exhibited a similar distribution as to what was observed in single labeling analysis (0.771 ± 0.031) (Fig. 5E–F). Statistical analysis revealed a significant difference in the distribution of MOR in DAMGO-treated groups compared to morphine- or vehicle-treated controls ($F(2,6)=21.94$, $p=0.0017$)(Fig. 6). The distribution of WLS following morphine was also significant compared to DAMGO and vehicle ($F(2,6)=24.01$, $p=0.0014$).

The morphine-induced shift in the distribution of WLS to the plasma membrane suggested that WLS may be present in proximity to the MOR on the plasma membrane. To examine the increased prevalence of MOR and WLS observed in close proximity at the plasma membrane (Fig. 5C–D and 6) the distance between large and small plasmalemmal particles

was measured in dual labeled morphine-treated dendritic profiles. When distributed along the plasma membrane, the mean distance between gold particles was 0.066 ± 0.007 microns. These data indicate that following morphine treatment, MOR and WLS occur in closer proximity on the plasma membrane, compared to the vehicle-treated animals (0.21 ± 0.03).

3.4 Exposure to heroin promotes formation of MOR/WLS complexes in locus coeruleus

To investigate the effect of opioid agonists on MOR/WLS complex formation, we used co-immunoprecipitation to determine whether opioid treatment promotes MOR/WLS complex formation in the LC. In these experiments, naïve male Sprague-Dawley rats were allowed one daily 150 minute heroin self-administration session for a period of 29 days (Grigson et al., unpublished). Each session consisted of three 40 minute drug access periods interspersed with two 15 minute periods of drug non-availability. During each 40 minute drug period, rats were allowed to self-administer heroin on a fixed ratio schedule (set number of licks on an active spout elicited one 0.06 mg/infusion dose of heroin). All subjects self-administered approximately an equal number of infusions of heroin over the course of the 29 days. Rats were then sacrificed, brains removed, and the LC dissected. Total cellular lysates were prepared from LCs of saline and heroin self-administering animals, and the MOR immunoprecipitated using an anti-MOR antibody. Immunocomplexes were then probed on Western blots for the presence of WLS with a chicken anti-WLS antibody (Jin et al., 2010a). As shown in Fig. 7A, WLS polypeptides migrate between 37 and 50 kDa (lysate lanes). The upper two bands represent glycosylated forms of WLS, whereas the 37 kDa band represents the WLS core protein (Jin et al., 2010b). MORs were associated with WLS under basal conditions (control IP lane) (Fig 7A–B), whereas MOR/WLS complex formation was significantly increased ($P < 0.05$) in the LC of rats with a history of having self-administered heroin (drug IP lanes) compared to control (Fig. 7A–B). These results are consistent with the idea that heroin, like morphine, increases MOR/WLS complex formation in the LC, presumably by causing redistribution of WLS from cytoplasm to the cell surface.

4. Discussion

The present study utilized high-resolution immunoelectron and confocal microscopy to demonstrate that (1) the MOR interacting protein, WLS, co-localized with MOR within TH-containing neurons in the LC; (2) following acute exposure to morphine, WLS shifts from a predominantly intracellular location to the plasma membrane where it is localized in close proximity to MOR; and (3) exposure to heroin promotes formation of MOR/WLS complexes in LC. Following morphine treatment, WLS is significantly re-distributed within the intracellular compartment compared to vehicle- and DAMGO-treated groups. Confirming previous reports, there was a significant internalization of MOR following DAMGO exposure when compared to vehicle and morphine treatment (Whistler and von Zastrow, 1999, Bailey et al., 2003, Reyes et al., 2010a, Reyes et al., 2011). Taken together, these data suggest that differential trafficking of WLS is induced by opiate agonists in noradrenergic LC neurons.

4.1 Technical Considerations

All antisera used in the present study have been well characterized and are specific to the antigen of interest. Briefly, the anti-WLS antibody was generated in chickens against a peptide antigen corresponding to the C-terminal 18 amino acids (HVDGPTEIYKLTRKEAQE) of human WLS, which is identical to the rat and mouse peptide sequence (Jin et al., 2010a). Antibodies of the IgY subtype were harvested from egg yolks and affinity purified prior to use. As demonstrated here, WLS recognized a single band of proteins with approximate molecular weight of about 50kDa (Jin et al., 2010b). Omission of the primary antibody abolished any detectable immunoreactivity (Reyes et al.,

2010a; Reyes et al., 2010b). Knockout validation of WLS antibodies was precluded by the embryonic lethality of homozygous null mutants (Fu et al., 2009). Both rabbit and guinea pig anti-MOR antibodies were directed against the C-terminal peptide of rat MOR. The specificity of these antisera were previously demonstrated through immunodot-blot analysis (Cheng et al., 1996), by the absence of immunoreactivity in adsorption control (Rodriguez et al., 2001, Drake and Milner, 2002), (Surratt et al., 1994), and in MOR KO mice (Jaferi and Pickel, 2009). The rate-limiting enzyme in norepinephrine synthesis, TH was used for the localization of LC noradrenergic neurons and this antisera has already been validated for specificity and characterization by previous studies in our group (Van Bockstaele and Pickel, 1993).

Pre-embedding immunogold-silver detection technique also has some limitations. This method provides superior subcellular localization of the antigen of interest while preserving optimal ultrastructural morphology (Leranth and Pickel, 1989a). The pre-embedding method is more appropriate than the post-embedding method for localization of immunoreactivity at extrasynaptic sites making quantification of MOR and WLS distribution more suitable (Lujan et al., 1996). A caveat of this approach, however, is that immunolabeling in thick sections prior to embedding can produce limited reagent penetration. In order to minimize issues of penetration 1) we collected tissue sections near the tissue-Epon interface where penetration of the antibody is optimal to ensure that immunolabeling was clearly detectable in sections included in the analysis (Chan et al., 1990), 2) profiles were sampled only when immunoreactivity was clearly present in sections included in the analysis, 3) sections were processed in parallel to facilitate relative comparisons (Reyes et al., 2010a), and a comparable number of dendritic profiles for each experimental animal was analyzed so that any limitation of the pre-embedding technique would not contribute to group differences. Although exposure to anesthetics during drug delivery has been shown to alter internalization of receptors, we did not see any evidence of this in the present study or in our previous work (Reyes et al., 2006, Reyes et al., 2008, Reyes et al., 2010b, Reyes et al., 2011). Vehicle-treated rats with similar anesthesia exposure did not show the same shift in subcellular distribution of MOR/WLS as drug exposed animals, suggesting that the use of anesthetics in our study did not confound the analysis.

4.2 Regulation of MOR by opioid agonists

The present study confirms previous studies showing that the internalization and trafficking of MOR is agonist dependent (Arden et al., 1995, Keith et al., 1996, Sternini et al., 1996, Keith et al., 1998, Whistler et al., 1999). As with other G-protein coupled receptors (GPCRs), MORs undergo desensitization, down-regulation and internalization in response to certain agonists (Bohm et al., 1997, Trapaidze et al., 2000, Tsao and von Zastrow, 2000, Kelly et al., 2008, Virk and Williams, 2008, Wang et al., 2008). The molecular processes underlying desensitization are thought to include rapid uncoupling of the receptor from its G proteins by phosphorylation of the receptor and/or binding of accessory proteins such as β-arrestins. Receptor internalization (loss of receptor from cell surface) has been implicated in the process of de-phosphorylation and re-sensitization of receptors (Tsao and von Zastrow, 2000).

Morphine does not show significant internalization (Kovoor et al., 1998), similar to heroin (Bohn et al., 2004). The inability of morphine or heroin to cause internalization has been implicated in the phenomenon of tolerance and dependence (Trapaidze et al., 2000, Zaki et al., 2000, Williams et al., 2001, Bohn et al., 2004). As receptor internalization may be a mechanism that mediates receptor turnover and re-sensitization, the inability of morphine to mediate this cellular response could result in chronic receptor activation that may engage intracellular signaling mechanisms causing downstream neuroadaptations.

4.3 Morphine-induced re-distribution of WLS in opiate sensitive LC neurons

The LC contains a high concentration of MORs (Van Bockstaele et al., 1996). MOR agonists inhibit the spontaneous activity of LC neurons via a pertussis toxin sensitive G-protein (Christie et al., 1986, Aghajanian and Wang, 1987, Christie et al., 1987a, Christie et al., 1987b, North et al., 1987, Curtis et al., 2001). Chronic morphine exposure increases TH expression (Guitart et al., 1990) while withdrawal from opiates, increases firing of LC neurons (Valentino and Wehby, 1989, Rasmussen et al., 1990, Kogan et al., 1992), and increases NE release in the forebrain (Rossetti et al., 1993). Consequently, physical symptoms develop that are NE-sensitive, as clonidine attenuates many aspects of the opiate withdrawal syndrome (Aghajanian, 1978, Silverstone et al., 1992). As approximately 70% of WLS and MOR are co-localized in TH-containing neurons in the LC, it is likely that chronic morphine exposure and withdrawal from opiates may engage these noradrenergic neurons containing WLS and MOR, however, further studies are needed to address this issue.

As a GPCR, MOR also has interacting proteins, called MORIPs that, through association, regulate activity and location of the receptor (Milligan, 2005, Georgoussi et al., 2012). WLS, a transmembrane protein and novel MORIP (Banziger et al., 2006, Jin et al., 2010a, Jin et al., 2010b, Reyes et al., 2010a, Reyes et al., 2011), has been identified within several brain regions, as well as in peripheral tissues, including skeletal muscle, heart muscle, lung, gut, liver and kidney (Jin et al., 2010a, Jin et al., 2010b). The present study provides evidence for localization of WLS in the LC and its re-distribution to the plasma membrane following morphine treatment. WLS was detected in both noradrenergic neurons as well as in neurons that lacked detectable TH immunoreactivity. These neurons may represent GABA interneurons that are known to be interdigitated with noradrenergic cells of the LC (Iijima et al., 1987, Van Bockstaele, 1998). In the present study, morphine and heroin exposure significantly increases association of WLS with MOR, consistent with prior studies (Jin et al., 2010; Reyes et al., 2011). WLS has been implicated in the chaperoning of Wnt glycoproteins from the endoplasmic reticulum to the plasma membrane where Wnts can be secreted (Banziger et al., 2006, Belenkaya et al., 2008, Franch-Marro et al., 2008, Port et al., 2008, Yang et al., 2008). Wnts are essential for a myriad of processes, including cell signaling, development, physiological processes (Logan and Nusse, 2004, Lie et al., 2005, Fu et al., 2009, Jin et al., 2010a). Based on yeast-two hybrid and GST-tagged immunoprecipitation evidence, WLS binds to and associates with MOR near the MOR intracellular loop two. This WLS-MOR binding requires residues in the WLS cytoplasmic tail (Jin et al., 2010a, Jin et al., 2010b) and may regulate MOR membrane localization. Thus, the interaction of WLS with MOR has functional implications for opiate actions in the LC. In fact, Johnson and colleagues (Johnson et al., 2006) reported that morphine-desensitized receptors are not internalized but are retained on the plasma membrane in the desensitized form as a result of different conformational changes of MORs being stabilized by different agonists that recruit different regulatory elements to the receptor. Furthermore, Ferguson (Ferguson, 2001) suggested that differences in internalization of specific GPCRs may be dictated by the complement of β-arrestin isoforms expressed in a cell. Specifically, within the LC, MORs are known to be differentially regulated by morphine and have been extensively characterized (Christie et al., 1987a, Beitner et al., 1989, Nestler et al., 1989, Valentino and Wehby, 1989, Van Bockstaele et al., 1996, Van Bockstaele and Commons, 2001, Van Bockstaele et al., 2001, Blanchet et al., 2003, Bailey et al., 2009a). Under basal conditions, endogenous opioids inhibit LC neuronal activity at the termination of a stressor to maintain homeostasis (Valentino et al., 1991, Curtis et al., 2001). Following morphine exposure the aforementioned inhibitory impact of MOR signaling is observed through activation of GIRKs to hyperpolarize LC neurons (Aghajanian and Wang, 1987, Blanchet et

al., 2003). Notably morphine does not cause rapid endocytosis of MOR (Keith et al., 1996, Kovoor et al., 1998, Van Bockstaele and Commons, 2001).

The difference in the degree of morphine-induced MOR endocytosis in the LC and other brain regions may be due to differential expression levels of internalization-related proteins, such as GRK2 and β-arrestins (Kelly, 2008). Morphine fails to induce MOR endocytosis in spinal cord in vivo (Trafton and Basbaum, 2004) and LC neurons in vitro (Arttamangkul et al., 2008) but induces endocytosis in the dendrites of medium spiny striatal neurons (Haberstock-Debic et al., 2003, 2005; Yu et al., 2009, 2010). These data suggest that morphine's actions on endocytosis may be different in different cell types and under different experimental conditions (Williams et al., 2013). Differences in patterns of internalization may be explained by the presence of morphine metabolites that are biased toward β-arrestin pathways (Frölich et al. (2011). In heterologous models over-expressing GRK2 or brain areas, such as the striatum, which contain high level of these proteins (GRK, beta-arrestins), this kinase effector system may enable morphine-induced MOR endocytosis (Bohn et al., 2004, Haberstock-Debic et al., 2005). Even within the striatum variability of GRK2 expression exists between specialized subpopulations of neurons (Bychkov, 2012) and beta-arrestin knockout mice have increased MOR signaling and reward responses (Bjork, 2013). The delicate balance between PKC membrane desensitization and GRK/beta-arrestin internalization pathways for MOR and the relative regulatory protein levels (GRK2, beta-arrestin-1 and −2) between the LC and striatum are increasingly complicated by nucleus-specific expression changes observed following acute, chronic, and withdrawal from morphine exposure (Fan, 2002; Fan, 2003). Considering the different roles of the striatum in extrapyramidal motor and habit learning (Calabresi, 1996; Graybiel, 1998; Graybiel, 2008; Kehagia, 2010; Cyriel, 2009) and the LC in processing of incoming afferent signals about the environment, respectively, discrepancies in their protein expression profile and response to morphine are not unexpected. Despite these differences the potential sequestration of MOR by WLS association at the plasma membrane is observed in both brain regions and suggests potential commonalities in signaling

We observed that following DAMGO treatment, WLS and MOR are both internalized and some of the internalized WLS is associated with endosome-like vesicles. Studies suggest that internalized WLS is normally degraded in lysosomes (Belenkaya et al., 2008; Yang et al., 2008); however, some internalized WLS escapes this fate and returns to the Golgi apparatus via the retromer complex which enables WLS re-utilization (Eaton, 2008). Similarly, DAMGO induces rapid internalization of MOR in striatal neurons when compared to morphine (Koch and Hollt, 2005). After internalization, endocytosed MORs return to the cell surface for renewed receptor activation and signaling (Haberstock-Debic et al., 2003; Haberstock-Debic, 2005). MOR trafficking in the striatum has been shown to be involved in the re-sensitization process (Roman-Vendrell et al., 2012). In the present study, our results show that DAMGO induces internalization of both WLS and MOR in LC neurons. Additional studies are required to determine the fate of internalized MOR/WLS following DAMGO exposure. When localized to the intracellular compartment, we also observed that immunogold labeling for WLS and MOR were in close proximity; however, we did not measure the distance between gold particles. Whether internalized WLS and MOR are associated within intracellular compartments following DAMGO exposure would be an interesting area to pursue.

Functional consequences of trafficking of WLS via association with MOR at the plasma membrane may serve to either limit WLS-mediated transport of Wnt secretion or facilitate its secretion. Decreasing Wnt secretion may potentially explain retraction, de-branching, and shrinking of dendrites following chronic morphine administration via depressed Wnt-induced dendritogenesis (Hu, 2008; Liao, 2007; Franch-Marro, 2008). Alternatively,

increased Wnt secretion may enable up-regulation of growth-related genes (McClung et al., 2005) or facilitate increased dendritogenesis enabling increased connections between afferents and LC dendrites such as under conditions of stress (Xu et al., 2004). Further studies are required to determine functional consequences of WLS trafficking. Finally, evidence from other studies suggest that GPCR interacting proteins may modulate GPCR trafficking in a regionally specific manner in pre-or postsynaptic plasma membranes. For example, PICK1, which associates with mGLUR7a, co-clusters at synaptic membranes selectively promoting receptor insertion at synapses on the pre-synaptic process (Boudin et al., 2000). Although the GluR2 subunit of the AMPA receptor is able to also associate with PICK1, the small (glutamate receptor interacting protein) GRIP 1 is uniquely required for synaptic localization of the receptor (Osten et al., 2000) and has been found to directly bind kinesins to direct the receptor to dendrites (Setou et al., 2002). Distal dendritic trafficking of the serotonin 5HT1A receptor similarly requires association with Yif1B, isolated from yeast (Carrel et al., 2008). The high specialization of this relationship despite the ubiquitous expression of Yifs is not unlike Rab1, which is also widespread and differentially traffics explicit classes of adrenergic receptors from the endoplasmic reticulum to the cell surface (Wu et al., 2003, Filipeanu et al., 2006). The possibility that MOR/WLS interactions may direct regionally specific insertion of MOR along specific compartments of the plasma membrane should be considered, especially considering the known chaperone and retromer complex paths of WLS near the intermediate compartment and Golgi complex (Franch-Marro et al., 2008).

5. Conclusion

Opiate addiction is a serious public health concern worldwide that claims numerous lives and accounts for a substantial financial burden. Uncovering the mechanisms of opiate exposure at the receptor level is crucial to the development of novel therapeutics for treatment. The present study utilized high-resolution immunoelectron and confocal microscopy to reveal abundant expression of WLS in noradrenergic neurons of the rat LC that are opiate-sensitive. Morphine caused WLS to shift from the cytoplasm to the plasma membrane where it was localized in close proximity to MOR. Heroin exposure induced an increased association MOR with WLS. Increased association of WLS/MOR may contribute to the negative downstream consequences of morphine on LC neurons. In summary, WLS may provide a novel target for therapeutic intervention in the treatment of opiate dependence.

Acknowledgments

This project was supported by the National Institutes of Health grant P20 DA #025995 and DA #05186 to W.H.B. and DA #009082 to E.V.B. This project was also funded, in part, by a grant from the Pennsylvania Department of Health using Tobacco CURE Funds to R.L. and P.S.G. The Department specifically disclaims responsibility for any analyses, interpretations or conclusions. We also would to thank Christain Njatcha and Dr. Bill Freeman expert technical assistance.

Abbreviations

WLS	Wntless
MOR	mu-opioid receptor
LC	locus coeruleus
NE	norepinephrine
DAMGO	[D-Ala2, N-Me-Phe4, Gly-ol5]-enkephalin

TH	tyrosine hydroxylase
GPCR	G-protein coupled receptor
GIP	G-protein interacting protein
MORIP	mu-opioid receptor interacting protein
i.c.v.	intracerebroventricular
PKC	protein kinase C
GRK	G-protein receptor kinase
GIRK	G-protein inwardly rectifying potassium channel
CREB	cAMP response element-binding protein

References

Aghajanian GK. Tolerance of locus coeruleus neurones to morphine and suppression of withdrawal response by clonidine. Nature. 1978; 276:186–188. [PubMed: 216919]

Aghajanian GK, Wang YY. Common alpha 2-and opiate effector mechanisms in the locus coeruleus: intracellular studies in brain slices. Neuropharmacology. 1987; 26:793–799. [PubMed: 2443865]

Arbilla S, Langer SZ. Morphine and beta-endorphin inhibit release of noradrenaline from cerebral cortex but not of dopamine from rat striatum. Nature. 1978; 9:559–561. [PubMed: 622192]

Arden JR, Segredo V, Wang Z, Lameh J, Sadee W. Phosphorylation and agonist-specific intracellular trafficking of an epitope-tagged mu-opioid receptor expressed in HEK 293 cells. J Neurochem. 1995; 65:1636–1645. [PubMed: 7561859]

Arttamangkul S, Torrecilla M, Kobayashi K, Okano H, Williams JT. Separation of mu-opioid receptor desensitization and internalization: endogenous receptors in primary neuronal cultures. J Neurosci. 2006; 26:4118–4125. [PubMed: 16611829]

Arttamangkul S, Quillinan N, Low MJ, von Zastrow M, Pintar J, Williams JT. Differential activation and trafficking of micro-opioid receptors in brain slices. Mol Pharmacol. 2008; 74:972–979. [PubMed: 18612077]

Aston-Jones G, Bloom FE. Activity of norepinephrine-containing locus coeruleus neurons in behaving rats anticipates fluctuations in the sleep-waking cycle. J Neurosci. 1981a; 1:876–886. [PubMed: 7346592]

Aston-Jones G, Bloom FE. Norepinephrine-containing locus coeruleus neurons in behaving rats exhibit pronounced responses to non-noxious environmental stimuli. J Neurosci. 1981b; 1:887–900. [PubMed: 7346593]

Aston-Jones G, Hirata H, Akaoka H. Local opiate withdrawal in locus coeruleus in vivo. Brain Res. 1997; 765:331–336. [PubMed: 9313908]

Bailey CP, Couch D, Johnson E, Griffiths K, Kelly E, Henderson G. Mu-opioid receptor desensitization in mature rat neurons: lack of interaction between DAMGO and morphine. J Neurosci. 2003; 23:10515–10520. [PubMed: 14627635]

Bailey CP, Kelly E, Henderson G. Protein kinase C activation enhances morphine-induced rapid desensitization of mu-opioid receptors in mature rat locus ceruleus neurons. Mol Pharmacol. 2004; 66:1592–1598. [PubMed: 15361548]

Bailey CP, Llorente J, Gabra BH, Smith FL, Dewey WL, Kelly E, Henderson G. Role of protein kinase C and mu-opioid receptor (MOPr) desensitization in tolerance to morphine in rat locus coeruleus neurons. Eur J Neurosci. 2009a; 29:307–318. [PubMed: 19200236]

Bailey CP, Oldfield S, Llorente J, Caunt CJ, Teschemacher AG, Roberts L, McArdle CA, Smith FL, Dewey WL, Kelly E, Henderson G. Involvement of PKC alpha and G-protein-coupled receptor kinase 2 in agonist-selective desensitization of mu-opioid receptors in mature brain neurons. Br J Pharmacol. 2009b; 158:157–164. [PubMed: 19309357]

Banziger C, Soldini D, Schutt C, Zipperlen P, Hausmann G, Basler K. Wntless, a conserved membrane protein dedicated to the secretion of Wnt proteins from signaling cells. Cell. 2006; 125:509–522. [PubMed: 16678095]

Bartscherer K, Pelte N, Ingelfinger D, Boutros M. Secretion of Wnt ligands requires Evi, a conserved transmembrane protein. Cell. 2006; 125:523–533. [PubMed: 16678096]

Beitner DB, Duman RS, Nestler EJ. A novel action of morphine in the rat locus coeruleus: persistent decrease in adenylate cyclase. Mol Pharmacol. 1989; 35:559–564. [PubMed: 2498635]

Belenkaya TY, Wu Y, Tang X, Zhou B, Cheng L, Sharma YV, Yan D, Selva EM, Lin X. The retromer complex influences Wnt secretion by recycling wntless from endosomes to the trans-Golgi network. Dev Cell. 2008; 14:120–131. [PubMed: 18160348]

Bermak JC, Li M, Bullock C, Zhou QY. Regulation of transport of the dopamine D1 receptor by a new membrane-associated ER protein. Nat Cell Biol. 2001; 3:492–498. [PubMed: 11331877]

Berridge CW, Waterhouse BD. The locus coeruleus-noradrenergic system: modulation of behavioral state and state-dependent cognitive processes. Brain Res Brain Res Rev. 2003; 42:33–84. [PubMed: 12668290]

Birdsong WT, Arttamangkul S, Clark MJ, Cheng K, Rice KC, Traynor JR, Williams JT. Increased agonist affinity at the mu-opioid receptor induced by prolonged agonist exposure. J Neurosci. 2013; 33:4118–4127. [PubMed: 23447620]

Bjork K, Tronci V, Thorsell A, Tanda G, Hirth N, Heilig M, Hansson AC, Sommer WH. beta-Arrestin 2 knockout mice exhibit sensitized dopamine release and increased reward in response to a low dose of alcohol. Psychopharmacology (Berl). 2013

Blanchet C, Sollini M, Luscher C. Two distinct forms of desensitization of G-protein coupled inwardly rectifying potassium currents evoked by alkaloid and peptide mu-opioid receptor agonists. Mol Cell Neurosci. 2003; 24:517–523. [PubMed: 14572471]

Blatchford KE, Diamond K, Westbrook RF, McNally GP. Increased vulnerability to stress following opiate exposures: behavioral and autonomic correlates. Behav Neurosci. 2005; 119:1034–1041. [PubMed: 16187831]

Blendy JA, Maldonado R. Genetic analysis of drug addiction: the role of cAMP response element binding protein. J Mol Med (Berl). 1998; 76:104–110. [PubMed: 9500675]

Bockaert J, Fagni L, Dumuis A, Marin P. GPCR interacting proteins (GIP). Pharmacol Ther. 2004; 103:203–221. [PubMed: 15464590]

Bockaert J, Marin P, Dumuis A, Fagni L. The ‘magic tail’ of G protein-coupled receptors: an anchorage for functional protein networks. FEBS Lett. 2003; 546:65–72. [PubMed: 12829238]

Bockaert J, Perroy J, Becamel C, Marin P, Fagni L. GPCR interacting proteins (GIPs) in the nervous system: Roles in physiology and pathologies. Annu Rev Pharmacol Toxicol. 2010; 50:89–109. [PubMed: 20055699]

Bohm A, Gaudet R, Sigler PB. Structural aspects of heterotrimeric G-protein signaling. Curr Opin Biotechnol. 1997; 8:480–487. [PubMed: 9265729]

Bohn LM, Dykstra LA, Lefkowitz RJ, Caron MG, Barak LS. Relative opioid efficacy is determined by the complements of the G protein-coupled receptor desensitization machinery. Mol Pharmacol. 2004; 66:106–112. [PubMed: 15213301]

Boudin H, Craig AM. Molecular determinants for PICK1 synaptic aggregation and mGluR7a receptor coclustering: role of the PDZ, coiled-coil, and acidic domains. J Biol Chem. 2001; 276:30270–30276. [PubMed: 11375398]

Boudin H, Doan A, Xia J, Shigemoto R, Huganir RL, Worley P, Craig AM. Presynaptic clustering of mGluR7a requires the PICK1 PDZ domain binding site. Neuron. 2000; 28:485–497. [PubMed: 11144358]

Bychkov E, Zurkovsky L, Garret MB, Ahmed MR, Gurevich EV. Distinct cellular and subcellular distributions of G protein-coupled receptor kinase and arrestin isoforms in the striatum. PloS One. 2012; 7(11):e48912. [PubMed: 23139825]

Calabresi P, Pisani A, Mercuri NB, Bernardi G. The corticostriatal projection: from synaptic plasticity to dysfunctions of the basal ganglia. Trends Neurosci. 1996; 19:19–24. [PubMed: 8787136]

Carrel D, Masson J, Al Awabdh S, Capra CB, Lenkei Z, Hamon M, Emerit MB, Darmon M. Targeting of the 5-HT1A serotonin receptor to neuronal dendrites is mediated by Yif1B. The Journal of neuroscience. 2008; 28:8063–8073. [PubMed: 18685031]

Castelli MP, Melis M, Mameli M, Fadda P, Diaz G, Gessa GL. Chronic morphine and naltrexone fail to modify mu-opioid receptor mRNA levels in the rat brain. Brain Res Mol Brain Res. 1997; 45:149–153. [PubMed: 9105683]

Ciani L, Salinas PC. WNTs in the vertebrate nervous system: from patterning to neuronal connectivity. Nat Rev Neurosci. 2005; 6:351–362. [PubMed: 15832199]

CDC, Center for Disease Control. CDC Grand Rounds: Prescription Drug Overdoses — a U.S. Epidemic. Morbidity and Mortality Weekly Report. 2012; 61:10–13. [PubMed: 22237030]

Chan J, Aoki C, Pickel VM. Optimization of differential immunogold-silver and peroxidase labeling with maintenance of ultrastructure in brain sections before plastic embedding. J Neurosci Methods. 1990; 33:113–127. [PubMed: 1977960]

Cheng PY, Moriwaki A, Wang JB, Uhl GR, Pickel VM. Ultrastructural localization of mu-opioid receptors in the superficial layers of the rat cervical spinal cord: extrasynaptic localization and proximity to Leu5-enkephalin. Brain Res. 1996; 731:141–154. [PubMed: 8883864]

Christie MJ. Cellular neuroadaptations to chronic opioids: tolerance, withdrawal and addiction. Br J Pharmacol. 2008; 154:384–396. [PubMed: 18414400]

Christie MJ, Williams JT, North RA. Tolerance to opioids in single locus coeruleus neurons of the rat. NIDA Res Monogr. 1986; 75:591–594. [PubMed: 3123980]

Christie MJ, Williams JT, North RA. Cellular mechanisms of opioid tolerance: studies in single brain neurons. Mol Pharmacol. 1987a; 32:633–638. [PubMed: 2824980]

Christie MJ, Williams JT, North RA. Mechanisms of tolerance to opiates in locus coeruleus neurons. NIDA Res Monogr. 1987b; 78:158–168. [PubMed: 2829019]

Ciani L, Salinas PC. WNTs in the vertebrate nervous system: from patterning to neuronal connectivity. Nat Rev Neurosci. 2005; 6:351–362. [PubMed: 15832199]

Connor M, Osborne PB, Christie MJ. Mu-opioid receptor desensitization: is morphine different? Br J Pharmacol. 2004; 143:685–696. [PubMed: 15504746]

Curtis AL, Bello NT, Valentino RJ. Evidence for functional release of endogenous opioids in the locus ceruleus during stress termination. J Neurosci. 2001; 21:RC152. [PubMed: 11406637]

Dang VC, Christie MJ. Mechanisms of rapid opioid receptor desensitization, resensitization and tolerance in brain neurons. Br J Pharmacol. 2012; 165:1704–1716. [PubMed: 21564086]

Doll C, Poll F, Peuker K, Loktev A, Gluck L, Schulz S. Deciphering micro-opioid receptor phosphorylation and dephosphorylation in HEK293 cells. Br J Pharmacol. 2012; 167:1259–1270. [PubMed: 22725608]

Drake CT, Milner TA. Mu opioid receptors are in discrete hippocampal interneuron subpopulations. Hippocampus. 2002; 12:119–136. [PubMed: 12000113]

Duman RS, Tallman JF, Nestler EJ. Acute and chronic opiate-regulation of adenylate cyclase in brain: specific effects in locus coeruleus. J Pharmacol Exp Ther. 1988; 246:1033–1039. [PubMed: 2843624]

Eaton S. Retromer retrieves wntless. Dev Cell. 2008; 14:4–6. [PubMed: 18194646]

Fan X, Zhang J, Zhang X, Yue W, Ma L. Acute and chronic morphine treatments and morphine withdrawal differentially regulate GRK2 and GRK5 gene expression in rat brain. Neuropharmacology. 2002; 43:809–816. [PubMed: 12384166]

Fan XL, Zhang JS, Zhang XQ, Yue W, Ma L. Differential regulation of beta-arrestin 1 and beta-arrestin 2 gene expression in rat brain by morphine. Neuroscience. 2003; 117:383–389. [PubMed: 12614678]

Ferguson SS. Evolving concepts in G protein-coupled receptor endocytosis: the role in receptor desensitization and signaling. Pharmacol Rev. 2001; 53:1–24. [PubMed: 11171937]

Filipeanu CM, Zhou F, Fugetta EK, Wu G. Differential regulation of the cell-surface targeting and function of β-and α1-adrenergic receptors by Rab1 GTPase in cardiac myocytes. Mol Pharmacol. 2006; 69:1571–1578. [PubMed: 16461589]

Fleming, WW.; Taylor, DA. Cellular mechanisms of opioid tolerance and dependence. In: Tseng, LR., editor. Pharmacology of Opioid Peptide. Amsterdam: Harwood Academic Publications; 1995. p. 463-502.

Foote SL, Aston-Jones G, Bloom FE. Impulse activity of locus coeruleus neurons in awake rats and monkeys is a function of sensory stimulation and arousal. Proc Natl Acad Sci U S A. 1980; 77:3033–3037. [PubMed: 6771765]

Foote SL, Bloom FE, Aston-Jones G. Nucleus locus ceruleus: new evidence of anatomical and physiological specificity. Physiol Rev. 1983; 63:844–914. [PubMed: 6308694]

Franch-Marro X, Wendler F, Guidato S, Griffith J, Baena-Lopez A, Itasaki N, Maurice MM, Vincent JP. Wingless secretion requires endosome-to-Golgi retrieval of Wntless/Evi/Sprinter by the retromer complex. Nat Cell Biol. 2008; 10:170–177. [PubMed: 18193037]

Frolich N, Dees C, Paetz C, Ren X, Lohse MJ, Nikolaev VO, Zenk MH. Distinct pharmacological properties of morphine metabolites at G(i)-protein and beta-arrestin signaling pathways activated by the human mu-opioid receptor. Biochem Pharmacol. 2012; 81:1248–1254. [PubMed: 21396918]

Fu J, Jiang M, Mirando AJ, Yu HM, Hsu W. Reciprocal regulation of Wnt and Gpr177/mouse Wntless is required for embryonic axis formation. Proc Natl Acad Sci U S A. 2009; 106:18598–18603. [PubMed: 19841259]

Funada M, Suzuki T, Sugano Y, Tsubai M, Misawa M, Ueda H, Misu Y. Role of beta-adrenoceptors in the expression of morphine withdrawal signs. Life Sci. 1994; 54:PL113–PL118. [PubMed: 7509021]

Georgoussi Z, Georganta EM, Milligan G. The other side of opioid receptor signalling: regulation by protein-protein interaction. Curr Drug Targets. 2012; 13:80–102. [PubMed: 21777181]

Gold MS, Redmond DE Jr, Kleber HD. Noradrenergic hyperactivity in opiate withdrawal supported by clonidine reversal of opiate withdrawal. Am J Psychiatry. 1979; 136:100–102. [PubMed: 364997]

Goodman OB Jr, Krupnick JG, Santini F, Gurevich VV, Penn RB, Gagnon AW, Keen JH, Benovic JL. Beta-arrestin acts as a clathrin adaptor in endocytosis of the beta2-adrenergic receptor. Nature. 1996; 383:447–450. [PubMed: 8837779]

Goodman RM, Thombre S, Firtina Z, Gray D, Betts D, Roebuck J, Spana EP, Selva EM. Sprinter: a novel transmembrane protein required for Wg secretion and signaling. Development. 2006; 133:4901–4911. [PubMed: 17108000]

Gordon, D.; Dahl, JL. Opioid Withdrawal 2nd edition. Fast Facts and Concepts-Meidcal College of Wisconsin; 2007.

Graybiel AM. The basal ganglia and chunking of action repertoires. Neurobiol Learn Mem. 1998; 70:119–136. [PubMed: 9753592]

Graybiel AM. Habits, rituals, and the evaluative brain. Annu Rev Neurosci. 2008; 31:359–387. [PubMed: 18558860]

Groer CE, Schmid CL, Jaeger AM, Bohn LM. Agonist-directed interactions with specific beta-arrestins determine mu-opioid receptor trafficking, ubiquitination, and dephosphorylation. J Biol Chem. 2011; 286:31731–31741. [PubMed: 21757712]

Guitart X, Hayward M, Nisenbaum LK, Beitner-Johnson DB, Haycock JW, Nestler EJ. Identification of MARPP-58, a morphine- and cyclic AMP-regulated phosphoprotein of 58 kDa, as tyrosine hydroxylase: evidence for regulation of its expression by chronic morphine in the rat locus coeruleus. J Neurosci. 1990; 10:2649–2659. [PubMed: 1974920]

Guitart X, Nestler EJ. Second messenger and protein phosphorylation mechanisms underlying opiate addiction: studies in the rat locus coeruleus. Neurochem Res. 1993; 18:5–13. [PubMed: 8385277]

Guitart X, Thompson MA, Mirante CK, Greenberg ME, Nestler EJ. Regulation of cyclic AMP response element-binding protein (CREB) phosphorylation by acute and chronic morphine in the rat locus coeruleus. J Neurochem. 1992; 58:1168–1171. [PubMed: 1531356]

Haberstock-Debic H, Kim KA, Yu YJ, von Zastrow M. Morphine promotes rapid, arrestin-dependent endocytosis of mu-opioid receptors in striatal neurons. J Neurosci. 2005; 25:7847–7857. [PubMed: 16120787]

Haberstock-Debic H, Wein M, Barrot M, Colago EE, Rahman Z, Neve RL, Pickel VM, Nestler EJ, von Zastrow M, Svingos AL. Morphine acutely regulates opioid receptor trafficking selectively in dendrites of nucleus accumbens neurons. J Neurosci. 2003; 23:4324–4332. [PubMed: 12764121]

Hannan MA, Kabbani N, Paspalas CD, Levenson R. Interaction with dopamine D2 receptor enhances expression of transient receptor potential channel 1 at the cell surface. Biochim Biophys Acta. 2008; 1778:974–982. [PubMed: 18261457]

Houshyar H, Galigniana MD, Pratt WB, Woods JH. Differential responsivity of the hypothalamic-pituitary-adrenal axis to glucocorticoid negative-feedback and corticotropin releasing hormone in rats undergoing morphine withdrawal: possible mechanisms involved in facilitated and attenuated stress responses. J Neuroendocrinol. 2001; 13:875–886. [PubMed: 11679056]

Hu F, Li G, Liang Z, Yang Y, Zhou Y. The morphological changes of pyramidal and spiny stellate cells in the primary visual cortex of chronic morphine treated cats. Brain Res Bull. 2008; 77:77–83. [PubMed: 18638530]

Hu LA, Tang Y, Miller WE, Cong M, Lau AG, Lefkowitz RJ, Hall RA. beta 1-adrenergic receptor association with PSD-95. Inhibition of receptor internalization and facilitation of beta 1-adrenergic receptor interaction with N-methyl-D-aspartate receptors. J Biol Chem. 2000; 275:38659–38666. [PubMed: 10995758]

Hull LC, Llorente J, Gabra BH, Smith FL, Kelly E, Bailey C, Henderson G, Dewey WL. The effect of protein kinase C and G protein-coupled receptor kinase inhibition on tolerance induced by mu-opioid agonists of different efficacy. J Pharmacol Exp Ther. 2010; 332:1127–1135. [PubMed: 20008489]

Iijima K, Kobayashi R, Kojima N. Immunohistochemical studies on GABAergic neurons in the rat locus coeruleus, with special reference to their relationship to astrocytes. Acta Anat (Basel). 1987; 129:116–122. [PubMed: 3307271]

Jaferi A, Pickel VM. Mu-opioid and corticotropin-releasing-factor receptors show largely postsynaptic co-expression, and separate presynaptic distributions, in the mouse central amygdala and bed nucleus of the stria terminalis. Neuroscience. 2009; 159:526–539. [PubMed: 19166913]

Jin J, Kittanakom S, Wong V, Reyes BA, Van Bockstaele EJ, Stagljar I, Berrettini W, Levenson R. Interaction of the mu-opioid receptor with GPR177 (Wntless) inhibits Wnt secretion: potential implications for opioid dependence. BMC Neurosci. 2010a; 11:33. [PubMed: 20214800]

Jin J, Morse M, Frey C, Petko J, Levenson R. Expression of GPR177 (Wntless/Evi/Sprinter), a highly conserved Wnt-transport protein, in rat tissues, zebrafish embryos, and cultured human cells. Dev Dyn. 2010b; 239:2426–2434. [PubMed: 20652957]

Johnson EA, Oldfield S, Braksator E, Gonzalez-Cuello A, Couch D, Hall KJ, Mundell SJ, Bailey CP, Kelly E, Henderson G. Agonist-selective mechanisms of mu-opioid receptor desensitization in human embryonic kidney 293 cells. Mol Pharmacol. 2006; 70:676–685. [PubMed: 16682505]

Karpa KD, Lidow MS, Pickering MT, Levenson R, Bergson C. N-linked glycosylation is required for plasma membrane localization of D5, but not D1, dopamine receptors in transfected mammalian cells. Mol Pharmacol. 1999; 56:1071–1078. [PubMed: 10531415]

Kehagia AA, Murray GK, Robbins TW. Learning and cognitive flexibility: frontostriatal function and monoaminergic modulation. Curr Opin Neurobiol. 2010; 20:199–204. [PubMed: 20167474]

Keith DE, Anton B, Murray SR, Zaki PA, Chu PC, Lissin DV, Monteillet-Agius G, Stewart PL, Evans CJ, von Zastrow M. mu-Opioid receptor internalization: opiate drugs have differential effects on a conserved endocytic mechanism in vitro and in the mammalian brain. Mol Pharmacol. 1998; 53:377–384. [PubMed: 9495801]

Keith DE, Murray SR, Zaki PA, Chu PC, Lissin DV, Kang L, Evans CJ, von Zastrow M. Morphine activates opioid receptors without causing their rapid internalization. J Biol Chem. 1996; 271:19021–19024. [PubMed: 8702570]

Kelly E, Bailey CP, Henderson G. Agonist-selective mechanisms of GPCR desensitization. Br J Pharmacol. 2008; 153(Suppl 1):S379–S388. [PubMed: 18059321]

Koch T, Hollt V. Role of receptor internalization in opioid tolerance and dependence. Pharmacol Ther. 2008; 117:199–206. [PubMed: 18076994]

Koch T, Widera A, Bartzsch K, Schulz S, Brandenburg LO, Wundrack N, Beyer A, Grecksch G, Hollt V. Receptor endocytosis counteracts the development of opioid tolerance. Mol Pharmacol. 2005; 67:280–287. [PubMed: 15475572]

Kogan JH, Nestler EJ, Aghajanian GK. Elevated basal firing rates and enhanced responses to 8-Br-cAMP in locus coeruleus neurons in brain slices from opiate-dependent rats. Eur J Pharmacol. 1992; 211:47–53. [PubMed: 1618268]

Koob GF, Maldonado R, Stinus L. Neural substrates of opiate withdrawal. Trends Neurosci. 1992; 15:186–191. [PubMed: 1377426]

Kovoor A, Celver JP, Wu A, Chavkin C. Agonist induced homologous desensitization of mu-opioid receptors mediated by G protein-coupled receptor kinases is dependent on agonist efficacy. Mol Pharmacol. 1998; 54:704–711. [PubMed: 9765514]

Lane-Ladd SB, Pineda J, Boundy VA, Pfeuffer T, Krupinski J, Aghajanian GK, Nestler EJ. CREB (cAMP response element-binding protein) in the locus coeruleus: biochemical, physiological, and behavioral evidence for a role in opiate dependence. J Neurosci. 1997; 17:7890–7901. [PubMed: 9315909]

Leranth, C.; Pickel, VM. Electron microscopic pre-embedding double immunostaining methods. N. In: Heimer, L.; Zaborsky, L., editors. euroanatomical tract-tracing methods II, recent progress. New York: Plenum; 1989a. p. 129-172.

Leranth, C.; Pickel, VM. Electron microscopic preembedding double-labeling methods. In: Heimer, L.; Zaborszky, L., editors. Neuroanatomical tracing methods. 1st ed. Vol. 2. New York: Plenum Press; 1989b. p. 129-172.

Liao D, Grigoriants OO, Wang W, Wiens K, Loh HH, Law PY. Distinct effects of individual opioids on the morphology of spines depend upon the internalization of mu opioid receptors. Mol Cell Neurosci. 2007; 35:456–469. [PubMed: 17513124]

Lie DC, Colamarino SA, Song HJ, Desire L, Mira H, Consiglio A, Lein ES, Jessberger S, Lansford H, Dearie AR, Gage FH. Wnt signalling regulates adult hippocampal neurogenesis. Nature. 2005; 437:1370–1375. [PubMed: 16251967]

Logan CY, Nusse R. The Wnt signaling pathway in development and disease. Annu Rev Cell Dev Biol. 2004; 20:781–810. [PubMed: 15473860]

Lujan R, Nusser Z, Roberts JD, Shigemoto R, Somogyi P. Perisynaptic location of metabotropic glutamate receptors mGluR1 and mGluR5 on dendrites and dendritic spines in the rat hippocampus. Eur J Neurosci. 1996; 8:1488–1500. [PubMed: 8758956]

Maldonado R, Stinus L, Gold LH, Koob GF. Role of different brain structures in the expression of the physical morphine withdrawal syndrome. J Pharmacol Exp Ther. 1992; 261:669–677. [PubMed: 1578378]

Maldonado R, Valverde O, Garbay C, Roques BP. Protein kinases in the locus coeruleus and periaqueductal gray matter are involved in the expression of opiate withdrawal. Naunyn Schmiedebergs Arch Pharmacol. 1995; 352:565–575. [PubMed: 8751087]

Martini L, Whistler JL. The role of mu opioid receptor desensitization and endocytosis in morphine tolerance and dependence. Curr Opin Neurobiol. 2007; 17:556–564. [PubMed: 18068348]

McClung CA, Nestler EJ, Zachariou V. Regulation of gene expression by chronic morphine and morphine withdrawal in the locus ceruleus and ventral tegmental area. J Neurosci. 2005; 25:6005–6015. [PubMed: 15976090]

Milligan G. Opioid receptors and their interacting proteins. Neuromolecular Med. 2005; 7:51–59. [PubMed: 16052038]

Montel H, Starke K, Taube HD. Morphine tolerance and dependence in noradrenaline neurones of the rat cerebral cortex. Naunyn Schmiedebergs Arch Pharmacol. 1975; 288:415–426. [PubMed: 1237093]

Moyse E, Marcel D, Leonard K, Beaudet A. Electron microscopic distribution of mu opioid receptors on noradrenergic neurons of the locus coeruleus. Eur J Neurosci. 1997; 9:128–139. [PubMed: 9042577]

Nestler EJ. Cellular responses to chronic treatment with drugs of abuse. Crit Rev Neurobiol. 1993; 7:23–39. [PubMed: 8385579]

Nestler EJ. Molecular basis of long-term plasticity underlying addiction. Nat Rev Neurosci. 2001; 2:119–128. [PubMed: 11252991]

Nestler EJ, Alreja M, Aghajanian GK. Molecular and cellular mechanisms of opiate action: studies in the rat locus coeruleus. Brain Res Bull. 1994; 35:521–528. [PubMed: 7859110]

Nestler EJ, Alreja M, Aghajanian GK. Molecular control of locus coeruleus neurotransmission. Biol Psychiatry. 1999; 46:1131–1139. [PubMed: 10560020]

Nestler EJ, Erdos JJ, Terwilliger R, Duman RS, Tallman JF. Regulation of G proteins by chronic morphine in the rat locus coeruleus. Brain Res. 1989; 476:230–239. [PubMed: 2495149]

Nestler EJ, Tallman JF. Chronic morphine treatment increases cyclic AMP-dependent protein kinase activity in the rat locus coeruleus. Mol Pharmacol. 1988; 33:127–132. [PubMed: 3340078]

Norgauer J, Eberle M, Fay SP, Lemke HD, Sklar LA. Kinetics of N-formyl peptide receptor up-regulation during stimulation in human neutrophils. J Immunol. 1991; 146:975–980. [PubMed: 1988505]

North RA, Williams JT, Surprenant A, Christie MJ. Mu and delta receptors belong to a family of receptors that are coupled to potassium channels. Proc Natl Acad Sci U S A. 1987; 84:5487–5491. [PubMed: 2440052]

Onoprishvili I, Andria ML, Kramer HK, Ancevska-Taneva N, Hiller JM, Simon EJ. Interaction between the mu opioid receptor and filamin A is involved in receptor regulation and trafficking. Mol Pharmacol. 2003; 64:1092–1100. [PubMed: 14573758]

Osten P, Khatri L, Perez JL, Köhr G, Giese G, Daly C, Schulz TW, Wensky A, Lee LM, Ziff EB. Mutagenesis reveals a role for ABP/GRIP binding to GluR2 in synaptic surface accumulation of the AMPA receptor. Neuron. 2000; 27:313–325. [PubMed: 10985351]

Page ME, Valentino RJ. Locus coeruleus activation by physiological challenges. Brain Res Bull. 1994; 35:557–560. [PubMed: 7859113]

Paxinos, G.; Watson, C. The rat brain in stereotaxic coordinates. New York: Academic Press; 1986.

Paxinos, G.; Watson, C. The Rat Brain in Stereotaxic Coordinates. San Diego, CA: Academic Press Inc; 1997.

Pennartz CM, Berke JD, Graybiel AM, Ito R, Lansink CS, van der Meer M, Redish AD, Smith KS, Voorn P. Corticostriatal Interactions during Learning, Memory Processing, and Decision Making. J Neurosci. 2009; 29:12831–12838. [PubMed: 19828796]

Pert CB, Kuhar MJ, Snyder SH. Autoradiograhic localization of the opiate receptor in rat brain. Life Sci. 1975; 16:1849–1853. [PubMed: 1152615]

Peters A, Palay SL. The morphology of synapses. J Neurocytol. 1996; 25:687–700. [PubMed: 9023718]

Peters, A.; Palay, SL.; Webster, HdF. The Fine Structure of the Nervous System. New York: Oxford UP; 1991.

Petko J, Justice-Bitner S, Jin J, Wong V, Kittanakom S, Ferraro TN, Stagljar I, Levenson R. MOR Is Not Enough: Identification of Novel mu-Opioid Receptor Interacting Proteins Using Traditional and Modified Membrane Yeast Two-Hybrid Screens. PLoS One. 2013; 8:e67608. [PubMed: 23840749]

Petruzzi R, Ferraro TN, Kurschner VC, Golden GT, Berrettini WH. The effects of repeated morphine exposure on mu opioid receptor number and affinity in C57BL/6J and DBA/2J mice. Life Sci. 1997; 61:2057–2064. [PubMed: 9366513]

Port F, Kuster M, Herr P, Furger E, Banziger C, Hausmann G, Basler K. Wingless secretion promotes and requires retromer-dependent cycling of Wntless. Nat Cell Biol. 2008; 10:178–185. [PubMed: 18193032]

Quillinan N, Lau EK, Virk M, von Zastrow M, Williams JT. Recovery from mu-opioid receptor desensitization after chronic treatment with morphine and methadone. J Neurosci. 2011; 31:4434–4443. [PubMed: 21430144]

Rasmussen K, Beitner-Johnson DB, Krystal JH, Aghajanian GK, Nestler EJ. Opiate withdrawal and the rat locus coeruleus: behavioral, electrophysiological, and biochemical correlates. J Neurosci. 1990; 10:2308–2317. [PubMed: 2115910]

Reyes AR, Levenson R, Berrettini W, Van Bockstaele EJ. Ultrastructural relationship between the mu opioid receptor and its interacting protein, GPR177, in striatal neurons. Brain Res. 2010a; 1358:71–80. [PubMed: 20813097]

Reyes BA, Chavkin C, Van Bockstaele EJ. Agonist-induced internalization of kappa-opioid receptors in noradrenergic neurons of the rat locus coeruleus. J Chem Neuroanat. 2010b; 40:301–309. [PubMed: 20884346]

Reyes BA, Fox K, Valentino RJ, Van Bockstaele EJ. Agonist-induced internalization of corticotropin-releasing factor receptors in noradrenergic neurons of the rat locus coeruleus. Eur J Neurosci. 2006; 23:2991–2998. [PubMed: 16819988]

Reyes BA, Glaser JD, Van Bockstaele EJ. Ultrastructural evidence for co-localization of corticotropin-releasing factor receptor and mu-opioid receptor in the rat nucleus locus coeruleus. Neurosci Lett. 2007; 413:216–221. [PubMed: 17194545]

Reyes BA, Vakharia K, Ferraro TN, Levenson R, Berrettini WH, Van Bockstaele EJ. Opiate agonist-induced re-distribution of Wntless, a mu-opioid receptor interacting protein, in rat striatal neurons. Exp Neurol. 2011

Reyes BA, Valentino RJ, Van Bockstaele EJ. Stress-induced intracellular trafficking of corticotropin-releasing factor receptors in rat locus coeruleus neurons. Endocrinology. 2008; 149:122–130. [PubMed: 17947354]

Ritter SL, Hall RA. Fine-tuning of GPCR activity by receptor-interacting proteins. Nat Rev Mol Cell Biol. 2009; 10:819–830. [PubMed: 19935667]

Rodriguez JJ, Mackie K, Pickel VM. Ultrastructural localization of the CB1 cannabinoid receptor in mu-opioid receptor patches of the rat Caudate putamen nucleus. J Neurosci. 2001; 21:823–833. [PubMed: 11157068]

Roman-Vendrell C, Yu YJ, Yudowski GA. Fast modulation of mu-opioid receptor (MOR) recycling is mediated by receptor agonists. J Biol Chem. 2013; 287:14782–14791. [PubMed: 22378794]

Rossetti ZL, Longu G, Mercuro G, Gessa GL. Extraneuronal noradrenaline in the prefrontal cortex of morphine-dependent rats: tolerance and withdrawal mechanisms. Brain Res. 1993; 609:316–320. [PubMed: 8508313]

Sagara T, Egashira H, Okamura M, Fujii I, Shimohigashi Y, Kanematsu K. Ligand recognition in mu opioid receptor: experimentally based modeling of mu opioid receptor binding sites and their testing by ligand docking. Bioorg Med Chem. 1996; 4:2151–2166. [PubMed: 9022978]

SAMHSA, Substance Abuse and Mental Health Services Administration. Results from the 2010 National Survey on Drug Use and Health: Summary of National Findings, NSDUH Series H-41, HHS Publication No. (SMA) 11-4658. Rockville, MD: 2011.

Sauliere-Nzeh, Ndong A.; Millot, C.; Corbani, M.; Mazeres, S.; Lopez, A.; Salome, L. Agonist-selective dynamic compartmentalization of human Mu opioid receptor as revealed by resolutive FRAP analysis. J Biol Chem. 2013; 285:14514–14520. [PubMed: 20197280]

Scavone JL, Van Bockstaele EJ. Mu-opioid receptor redistribution in the locus coeruleus upon precipitation of withdrawal in opiate-dependent rats. Anat Rec (Hoboken). 2009; 292:401–411. [PubMed: 19248160]

Osten P, Khatri L, Perez JL, Köhr G, Giese G, Daly C, Schulz TW, Wensky A, Lee LM, Ziff EB. Mutagenesis reveals a role for ABP/GRIP binding to GluR2 in synaptic surface accumulation of the AMPA receptor. Neuron. 2000; 27:313–325. [PubMed: 10985351]

Setou M, Seog D-H, Tanaka Y, Kanai Y, Takei Y, Kawagishi M, Hirokawa N. Glutamate-receptor-interacting protein GRIP1 directly steers kinesin to dendrites. Nature. 2002; 417:83–87. [PubMed: 11986669]

Sharma SK, Klee WA, Nirenberg M. Opiate-dependent modulation of adenylate cyclase. Proc Natl Acad Sci U S A. 1977; 74:3365–3369. [PubMed: 269396]

Silverstone PH, Done C, Sharp T. Clonidine but not nifedipine prevents the release of noradrenaline during naloxone-precipitated opiate withdrawal: an in vivo microdialysis study in the rat. Psychopharmacology (Berl). 1992; 109:235–238. [PubMed: 1365663]

Simonin F, Karcher P, Boeuf JJ, Matifas A, Kieffer BL. Identification of a novel family of G protein-coupled receptor associated sorting proteins. J Neurochem. 2004; 89:766–775. [PubMed: 15086532]

Sternini C, Spann M, Anton B, Keith DE Jr, Bunnett NW, von Zastrow M, Evans C, Brecha NC. Agonist-selective endocytosis of mu opioid receptor by neurons in vivo. Proc Natl Acad Sci U S A. 1996; 93:9241–9246. [PubMed: 8799185]

Surratt CK, Johnson PS, Moriwaki A, Seidleck BK, Blaschak CJ, Wang JB, Uhl GR. -mu opiate receptor. Charged transmembrane domain amino acids are critical for agonist recognition and intrinsic activity. J Biol Chem. 1994; 269:20548–20553. [PubMed: 8051154]

Talbot JN, Skifter DA, Bianchi E, Monaghan DT, Toews ML, Murrin LC. Regulation of mu opioid receptor internalization by the scaffold protein RanBPM. Neurosci Lett. 2009; 466:154–158. [PubMed: 19788913]

Tempel A, Crain SM, Peterson ER, Simon EJ, Zukin RS. Antagonist-induced opiate receptor upregulation in cultures of fetal mouse spinal cord-ganglion explants. Brain Res. 1986; 390:287–291. [PubMed: 3006869]

Trapaidze N, Gomes I, Cvejic S, Bansinath M, Devi LA. Opioid receptor endocytosis and activation of MAP kinase pathway. Brain Res Mol Brain Res. 2000; 76:220–228. [PubMed: 10762697]

Tsao P, von Zastrow M. Downregulation of G protein-coupled receptors. Curr Opin Neurobiol. 2000; 10:365–369. [PubMed: 10851176]

United States Department of Justice National Drug Intelligence Center. The Economic Impact of Illicit Drug Use on American Society. In: NDIC. , editor. United States Department of Justice. Washington D.C.: 2011.

UNODC United Nations Office on Drugs and Crime. World Drug Report 2012. Vienna: United Nations Publication; 2012.

Valentino RJ, Page ME, Curtis AL. Activation of noradrenergic locus coeruleus neurons by hemodynamic stress is due to local release of corticotropin-releasing factor. Brain Res. 1991; 555:25–34. [PubMed: 1933327]

Valentino RJ, Wehby RG. Locus ceruleus discharge characteristics of morphine-dependent rats: effects of naltrexone. Brain Res. 1989; 488:126–134. [PubMed: 2743108]

Van Bockstaele EJ. Morphological substrates underlying opioid, epinephrine and gamma-aminobutyric acid inhibitory actions in the rat locus coeruleus. Brain Res Bull. 1998; 47:1–15. [PubMed: 9766384]

Van Bockstaele EJ, Colago EE, Cheng P, Moriwaki A, Uhl GR, Pickel VM. Ultrastructural evidence for prominent distribution of the mu-opioid receptor at extrasynaptic sites on noradrenergic dendrites in the rat nucleus locus coeruleus. J Neurosci. 1996; 16:5037–5048. [PubMed: 8756434]

Van Bockstaele EJ, Commons KG. Internalization of mu-opioid receptors produced by etorphine in the rat locus coeruleus. Neuroscience. 2001; 108:467–477. [PubMed: 11738260]

Van Bockstaele EJ, Menko AS, Drolet G. Neuroadaptive responses in brainstem noradrenergic nuclei following chronic morphine exposure. Mol Neurobiol. 2001; 23:155–171. [PubMed: 11817217]

Van Bockstaele EJ, Pickel VM. Ultrastructure of serotonin-immunoreactive terminals in the core and shell of the rat nucleus accumbens: cellular substrates for interactions with catecholamine afferents. J Comp Neurol. 1993; 334:603–617. [PubMed: 8408768]

Virk MS, Williams JT. Agonist-specific regulation of mu-opioid receptor desensitization and recovery from desensitization. Mol Pharmacol. 2008; 73:1301–1308. [PubMed: 18198283]

von Zastrow M, Svingos A, Haberstock-Debic H, Evans C. Regulated endocytosis of opioid receptors: cellular mechanisms and proposed roles in physiological adaptation to opiate drugs. Curr Opin Neurobiol. 2003; 13:348–353. [PubMed: 12850220]

Wang Y, Van Bockstaele EJ, Liu-Chen LY. In vivo trafficking of endogenous opioid receptors. Life Sci. 2008; 83:693–699. [PubMed: 18930741]

Wang Y, Xu W, Huang P, Chavkin C, Van Bockstaele EJ, Liu-Chen LY. Effects of acute agonist treatment on subcellular distribution of kappa opioid receptor in rat spinal cord. J Neurosci Res. 2009; 87:1695–1702. [PubMed: 19130621]

Whistler JL, Chuang HH, Chu P, Jan LY, von Zastrow M. Functional dissociation of mu opioid receptor signaling and endocytosis: implications for the biology of opiate tolerance and addiction. Neuron. 1999; 23:737–746. [PubMed: 10482240]

Whistler JL, von Zastrow M. Morphine-activated opioid receptors elude desensitization by beta-arrestin. Proc Natl Acad Sci U S A. 1998; 95:9914–9919. [PubMed: 9707575]

Whistler JL, von Zastrow M. Dissociation of functional roles of dynamin in receptor-mediated endocytosis and mitogenic signal transduction. J Biol Chem. 1999; 274:24575–24578. [PubMed: 10455121]

Widnell KL, Russell DS, Nestler EJ. Regulation of expression of cAMP response element-binding protein in the locus coeruleus in vivo and in a locus coeruleus-like cell line in vitro. Proc Natl Acad Sci U S A. 1994; 91:10947–10951. [PubMed: 7971989]

Williams JT, Christie MJ, Manzoni O. Cellular and synaptic adaptations mediating opioid dependence. Physiol Rev. 2001; 81:299–343. [PubMed: 11152760]

Williams JT, Ingram SL, Henderson G, Chavkin C, von Zastrow M, Schulz S, Koch T, Evans CJ, Christie MJ. Regulation of mu-opioid receptors: desensitization, phosphorylation, internalization, and tolerance. Pharmacol Rev. 2013; 65:223–254. [PubMed: 23321159]

Xia Z, Gray JA, Compton-Toth BA, Roth BL. A direct interaction of PSD-95 with 5-HT2A serotonin receptors regulates receptor trafficking and signal transduction. J Biol Chem. 2003; 278:21901–21908. [PubMed: 12682061]

Xu GP, Van Bockstaele E, Reyes B, Bethea T, Valentino RJ. Chronic morphine sensitizes the brain norepinephrine system to corticotropin-releasing factor and stress. J Neurosci. 2004; 24:8193–8197. [PubMed: 15385601]

Yang PT, Lorenowicz MJ, Silhankova M, Coudreuse DY, Betist MC, Korswagen HC. Wnt signaling requires retromer-dependent recycling of MIG-14/Wntless in Wnt-producing cells. Dev Cell. 2008; 14:140–147. [PubMed: 18160347]

Yi H, Leunissen J, Shi G, Gutekunst C, Hersch S. A novel procedure for pre-embedding double immunogold-silver labeling at the ultrastructural level. J Histochem Cytochem. 2001; 49:279–284. [PubMed: 11181730]

Yu Y, Zhang L, Yin X, Sun H, Uhl GR, Wang JB. Mu opioid receptor phosphorylation, desensitization, and ligand efficacy. J Biol Chem. 1997; 272:28869–28874. [PubMed: 9360954]

Wu G, Zhao G, He Y. Distinct Pathways for the Trafficking of Angiotensin II and Adrenergic Receptors from the Endoplasmic Reticulum to the Cell Surface Rab1-INDEPENDENT TRANSPORT OF AG PROTEIN-COUPLED RECEPTOR. Journal of Biological Chemistry. 2003; 278:47062–47069. [PubMed: 12970354]

Zaki PA, Keith DE Jr, Brine GA, Carroll FI, Evans CJ. Ligand-induced changes in surface mu-opioid receptor number: relationship to G protein activation? J Pharmacol Exp Ther. 2000; 292:1127–1134. [PubMed: 10688632]

Zheng H, Chu J, Zhang Y, Loh HH, Law PY. Modulating micro-opioid receptor phosphorylation switches agonist-dependent signaling as reflected in PKCepsilon activation and dendritic spine stability. J Biol Chem. 2011; 286:12724–12733. [PubMed: 21292762]

Zigmond SH, Sullivan SJ, Lauffenburger DA. Kinetic analysis of chemotactic peptide receptor modulation. J Cell Biol. 1982; 92:34–43. [PubMed: 6276415]

Highlights

- Immunohistochemistry and western blot analysis revealed robust WLS expression within the LC, the main source of norepinephrine to the forebrain.
- Using confocal and immunoelectron microscopy, robust co-localization of WLS and MOR was identified in noradrenergic neurons of the LC.
- WLS immunoreactivity shifts from the cytoplasm to plasma membrane following morphine treatment.
- Increased plasmalemmal association of WLS with MOR following morphine may result in sequestration of WLS and inhibition of Wnt protein secretion.
- Following heroin exposure, co-immunoprecipitation showed that WLS and MOR interact, and that WLS expression is altered.

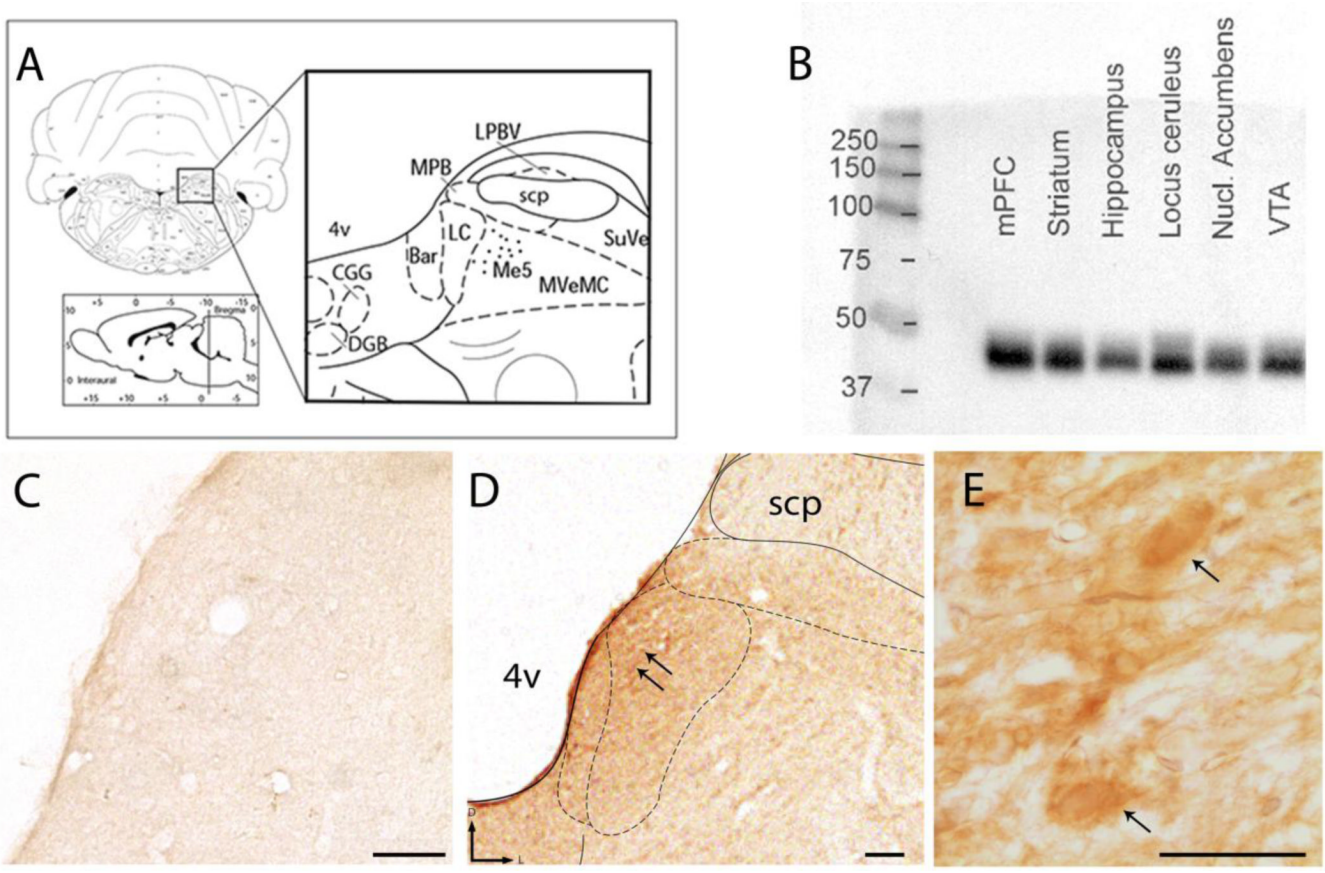

Figure 1.

Evidence for localization of WLS in the brainstem nucleus locus coeruleus. **A**) Representative schematic diagram adapted from the rat brain atlas of Paxinos and Watson at level bregma −10.03mm, plate 58, showing the regional localization of the LC in the dorsal pons (Paxinos, 1997). **B)** Western blot analysis shows WLS expression in whole cell lysates obtained from the medial prefrontal cortex (mPFC), striatum, hippocampus, locus coeruleus, nucleus (Nucl) accumbens and ventral tegmental area (VTA). A specific band in the 37–50kD range, the predicted molecular weight of WLS, can be observed in many brain regions, as previously reported. **C**) A tissue section through the dorsal pons that was processed in the absence of the primary antibody reveals a lack of immunoperoxidase staining. **D and E)** Immunoperoxidase labeling for WLS (black arrows) can be observed in the LC at low and high magnification. superior cerebellar peduncle, scp. 4v: 4th ventricle, scale bar 50 microns in **C-D**; 10 microns in **E**.

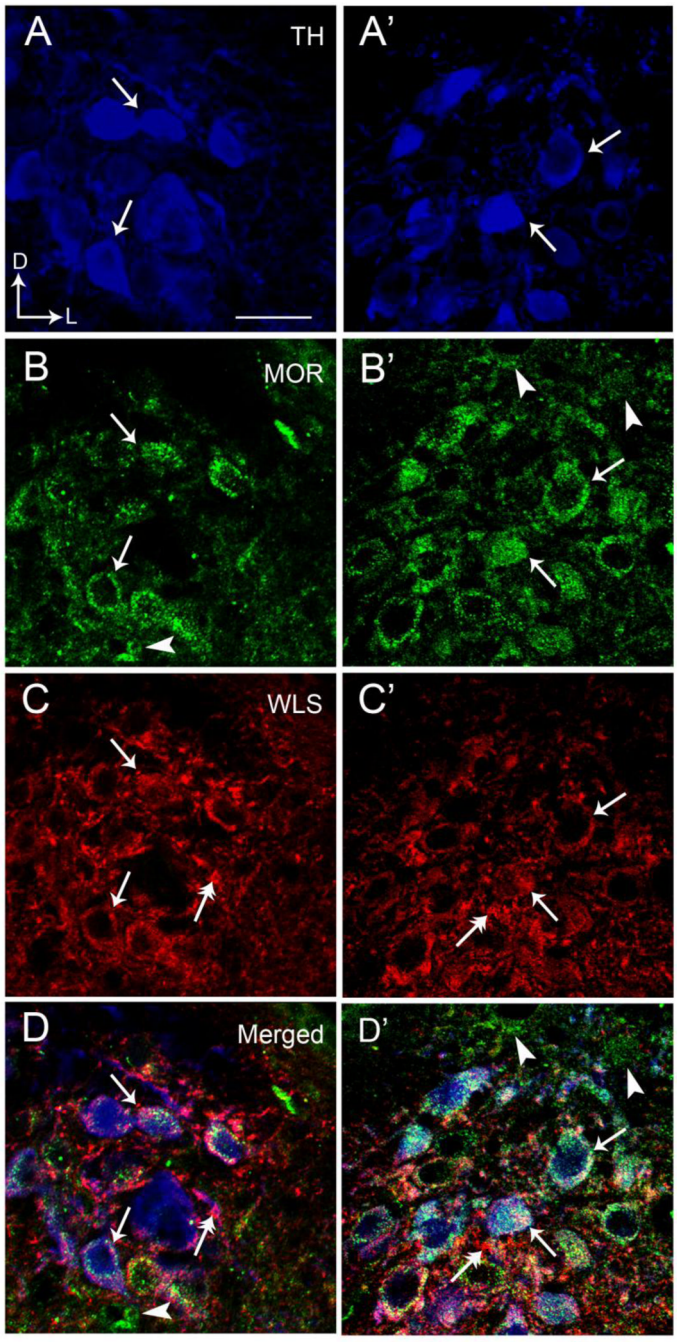

Figure 2.

High magnification immunofluorescence microscopy depicting colocalization of TH, MOR, and WLS in individual rat locus coeruleus (LC) neurons. **A** and **A'** illustrate MOR labeling (green) in the LC, **B** and **B'** show WLS labeling (red) and **C** and **C'** depict TH labeling (blue) in the same tissue. **D** and **D'** represent merged images for all three labels. Solid single black arrows indicate neurons that contain MOR, WLS and TH while arrowheads depict neurons containing only MOR. Dual headed arrows indicate neurons that only contain WLS. Arrows indicate dorsal (D) and lateral (L) orientation of the sections illustrated. Scale bar 20 microns.

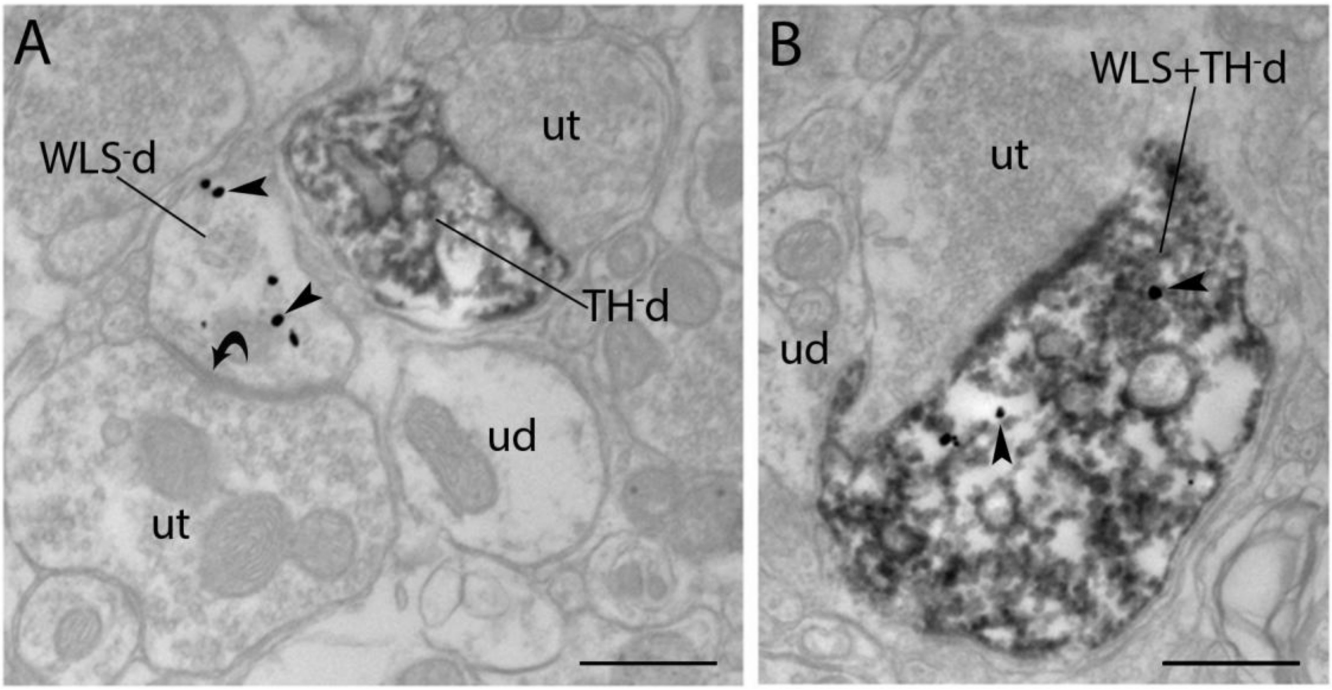

Figure 3.

Electron microscopic evidence for localization of WLS in rat noradrenergic dendrites of the locus coeruleus (LC). **A**) An immunoperoxidase labeled tyrosine hydroxylase dendrite (TH-d) is shown in proximity to an immunogold-silver labeled (arrowheads) WLS dendrite (WLS-d). The singly labeled dendrites receive direct symmetric synaptic contacts (curved arrows) from unlabeled axon terminals (ut). **B**) A dendrite contains both immunoperoxidase labeling for TH and immunogold-silver labeling (arrowheads) for WLS (WLS + TH-d). ud: unlabeled dendrites Scale bar 0.5 microns.

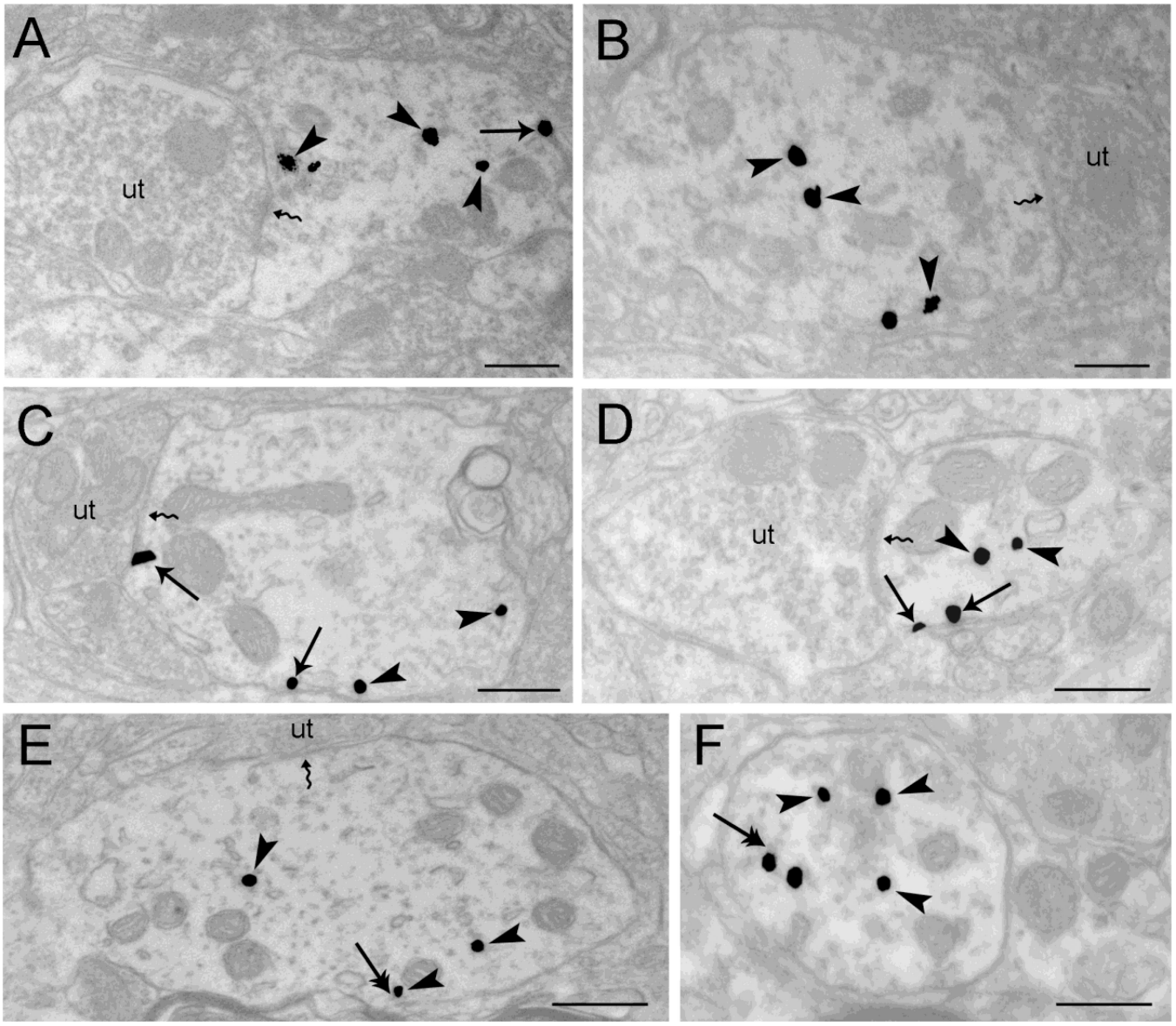

Figure 4.

Electron microscopic evidence for agonist-induced trafficking of WLS in rat locus coeruleus (LC) neurons using single immunogold-silver labeling for WLS. **A-B**. Sections from vehicle-treated subjects show immunogold-silver grains for WLS within the cytoplasm (arrowheads) and along the plasma membrane (arrow). Note that WLS is distributed both within the cytoplasm of dendrites as well as associated occasionally with the plasma membrane. Unlabeled axon terminals (ut) are shown contacting (zigzag arrows) the WLS-containing dendrite **C-D**. WLS immunolabeling shows a shift in distribution from the cytoplasm (arrowheads) to the plasma membrane (arrows) following morphine treatment. An unlabeled axon terminal (ut) is contacting (zigzag arrow) the WLS-containing dendrite. **E-F**. Following DAMGO treatment, immunogold-silver labeling for WLS (arrowheads) is primarily distributed within the cytoplasm. Double arrows point to endosome-like vesicles. An unlabeled axon terminal (ut) is shown contacting (zigzag arrow) the WLS-containing dendrite (Panel E). Scale bars, 0.5μm.

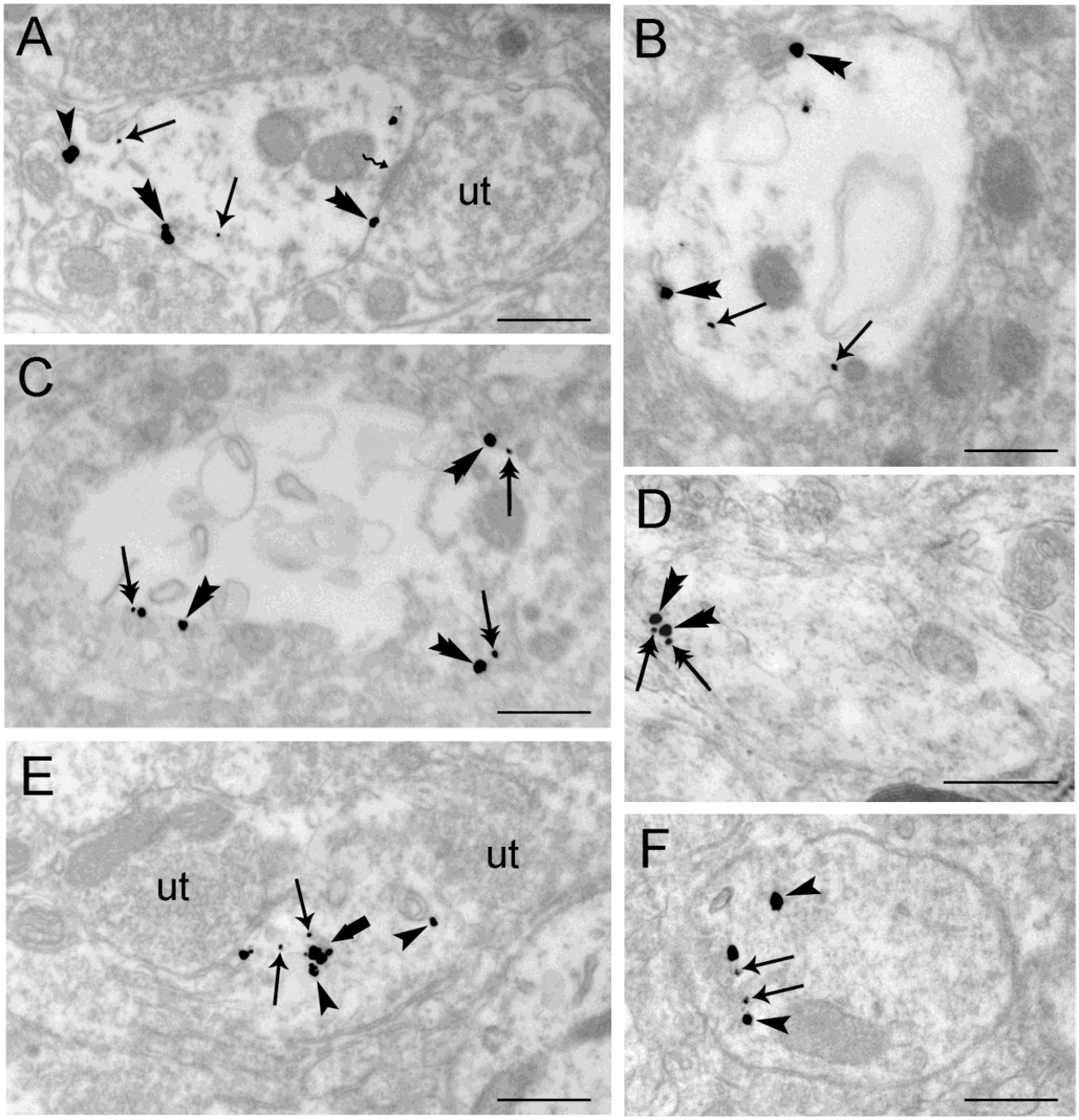

Figure 5.

Differential trafficking of WLS is observed in rat locus coeruleus (LC) dendrites from vehicle-treated (A, B), morphine-treated (C–D) and DAMGO-treated rats (E–F) using dual immunogold-silver for WLS (small gold-silver grains) and MOR (large gold-silver grains). **A-B**. Immunogold-silver labeling for WLS can be seen within the cytoplasm (arrows) while immunogold-silver labeling for MOR is distributed within the cytoplasm (arrowhead) and along the plasma membrane (double arrowheads) in dendrites from vehicle-treated rats. Panel A shows an unlabeled axon terminal (ut) contacting (zigzag arrow) the WLS and MOR-containing dendrite. **C-D**. Following morphine treatment, WLS labeling shifts from

the cytoplasm to the plasma membranes of LC dendrites. Double arrows point to immunogold-silver labeling for WLS along the plasma membranes while double arrowheads point to immunogold-silver for MOR labeling along the plasma membrane in WLS and MOR-containing dendrite. **E-F**. Immunogold-silver labeling for WLS (arrows) and MOR (arrowheads) can be seen primarily within the cytoplasm of the WLS and MOR-containing dendrites in rats subjected to DAMGO treatment. Two unlabeled axon terminals (ut) can be seen contacting a WLS and MOR-containing dendrite (Panel E). A thick arrow points to endosome-like vesicles. Scale bars, 0.5μm.

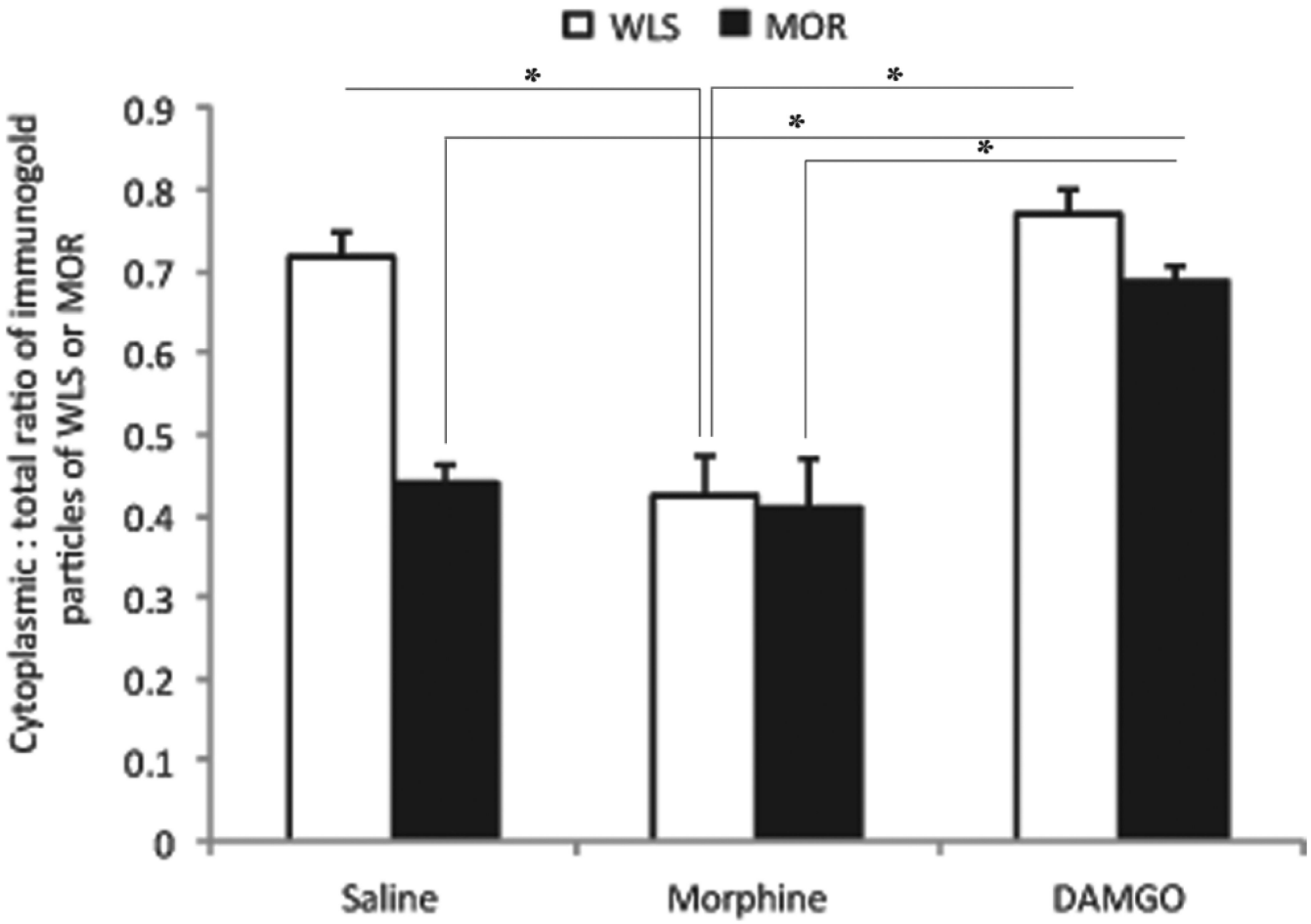

Figure 6.

Ratio of cytoplasmic to total immunogold–silver labeling for WLS and MOR following opiate agonist treatment. Morphine treatment caused a significant ($P < 0.05$) shift in WLS from the cytoplasmic compartment to the plasma membrane, while MOR remains on the plasma membrane, similar to control. DAMGO treatment significantly increased ($P < 0.05$) the ratio of cytoplasmic to total WLS immunogold–silver labeling compared to control and morphine treatment. DAMGO also caused a significant shift in MOR distribution to the cytoplasm compared to morphine and control. Values are mean ± SEM of three rats per group. Values with asterisks are significantly different (*$P < 0.05$) from each other. Tukey's multiple comparison tests after ANOVA.

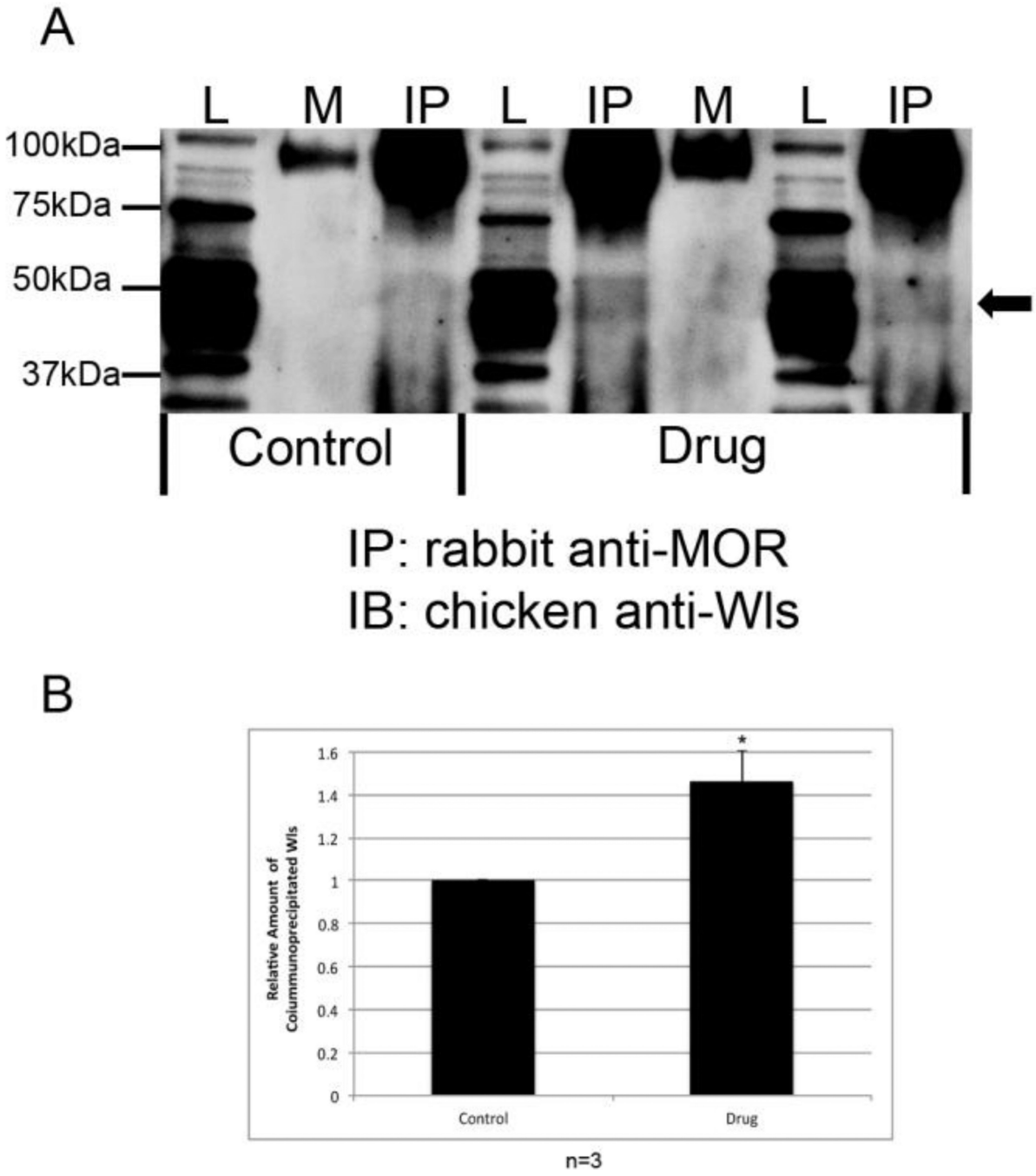

Figure 7.

Interaction of MOR and WLS in the locus coeruleus (LC) of saline and heroin self-administering rats. **(A)** MOR was immunoprecipitated (IP) from the LC of saline (control) and heroin (drug) self-administering rats using a rabbit anti-MOR antibody. Equal amounts of protein from LC tissue were added to each immunoprecipitation reaction. Interaction with WLS was determined by immunoblotting (IB) with a chicken anti-WLS antibody. Lysate (L) lanes contain 1% of the total protein from the LC compared to the mock (M, rabbit IgG) and immunoprecipitation (IP) lanes. Arrow indicates position of WLS. IgG heavy chain migrates as a dimer at ∼100 kDa. (B) Bands were analyzed by densitometry and quantified

using Image J software. Data was analyzed using paired Student's t-test (expressed as a mean ± SEM; n=3, (*$P < 0.05$).